

Validated forward integration scheme for parabolic PDEs via Chebyshev series

Jacek Cyranka ^{*}

Jean-Philippe Lessard[†]

Abstract

In this paper we introduce a new approach to compute rigorously solutions of Cauchy problems for a class of semi-linear parabolic partial differential equations. Expanding solutions with Chebyshev series in time and Fourier series in space, we introduce a zero finding problem $F(a) = 0$ on a Banach algebra X of Fourier-Chebyshev sequences, whose solution solves the Cauchy problem. The challenge lies in the fact that the linear part $\mathcal{L} \stackrel{\text{def}}{=} DF(0)$ has an infinite block diagonal structure with blocks becoming less and less diagonal dominant at infinity. We introduce analytic estimates to show that \mathcal{L} is a boundedly invertible linear operator on X , and we obtain explicit, rigorous and computable bounds for the operator norm $\|\mathcal{L}^{-1}\|_{B(X)}$. These bounds are then used to verify the hypotheses of a Newton-Kantorovich type argument which shows that the (Newton-like) operator $\mathcal{T}(a) \stackrel{\text{def}}{=} a - \mathcal{L}^{-1}F(a)$ is a contraction on a small ball centered at a numerical approximation of the Cauchy problem. The contraction mapping theorem yields a fixed point which corresponds to a classical (strong) solution of the Cauchy problem. The approach is simple to implement, numerically stable and is applicable to a class of PDE models, which include for instance Fisher's equation, the Kuramoto-Sivashinsky equation, the Swift-Hohenberg equation and the phase-field crystal (PFC) equation. We apply our approach to each of these models and report plausible experimental results, which motivate further research on the method.

Keywords: forward integration, parabolic PDE, Chebyshev series, Newton-Kantorovich, rigorous numeric

MSC: Primary: 65M99, Secondary: 65G20, 65M70, 65Y20

1 Introduction

In this paper, we introduce a new validated forward integration scheme for a class of parabolic partial differential equations (PDEs) based on Chebyshev expansion in time. The class of PDE problems we consider are Cauchy problems associated to dissipative semi-linear equations of the form

$$u_t = Lu + \partial_x^n N(u), \quad u(0, x) = u_0(x) \tag{1}$$

where $u = u(t, x) \in \mathbb{R}$, $u_0(x)$ is a given initial condition, $x \in \mathbb{T} = \mathbb{R}/2\pi$, $t \geq 0$, $\partial_x^\ell = \frac{\partial^\ell}{\partial x^\ell}$, $L = \sum_{\ell=0}^d \alpha_\ell \partial_x^\ell$ ($\alpha_\ell \in \mathbb{R}$) is a linear differential operator of *even* order d and N is a polynomial. We supplement model (1) with odd ($u(t, -x) = -u(t, x)$) or even ($u(t, -x) = u(t, x)$) boundary conditions. Moreover, we make the assumption that

$$d - 3n \geq 0 \tag{2}$$

^{*}University of Warsaw, Institute of Informatics, Stefana Banacha 2, 02-097 Warszawa, Poland. jcyranka@gmail.com

[†]McGill University, Department of Mathematics and Statistics, 805 Sherbrooke Street West, Montreal, Québec H3A 0B9, Canada. jp.lessard@mcgill.ca

which, roughly speaking, ensures that the representation of the operator $(\partial_x^n)^{-1}(\partial_t - L)$ is a boundedly invertible linear operator on a weighed ℓ^1 sequence space of Fourier-Chebyshev coefficients (see Section 3). While assumption (2) is restrictive, it is satisfied by known models like Fisher's equation ($d = 2, n = 0$, see Section 5.2), the Kuramoto-Sivashinsky equation ($d = 4, n = 1$, see Section 5.3), the Swift-Hohenberg equation ($d = 4, n = 0$, see Section 5.4), the phase-field crystal equation ($d = 6, n = 2$, see Section 5.5) and many others.

It is worth mentioning that the development of rigorous computational methods to study the flow of dissipative PDEs has received its fair share of attention in the last fifteen years. Let us mention the topological method based on covering relations and self-consistent bounds [1, 2, 3, 4, 5, 6, 7], the C^1 rigorous integrator of [8], the semi-group approach of [9, 10, 11, 12], and the finite element discretization based approach of [13, 14, 15]. This interest is perhaps not surprising as dissipative PDEs naturally lead to the notion of infinite-dimensional dynamical systems in the form of semi-flows, and understanding the asymptotic and bounded dynamics of these models is strongly facilitated by a rigorous investigation of the flow. While rigorous computations of periodic orbits may avoid the necessity of computing the flow (they can indeed be obtained with Fourier expansions in time [16, 17, 18, 19]), solutions to boundary values problems or connecting orbits often require computing the semi-flow. In this paper, we introduce a new validated numerical method to compute solutions of Cauchy problems, which we now briefly describe.

Our approach goes as follows. Expand the solution $u(t, x)$ as a Fourier series in x with time-dependent Fourier coefficients. Obtain an infinite system of nonlinear ordinary differential equations (ODEs) to be solved on a time interval $[0, h]$. Using the Fourier coefficients of the initial condition $u_0(x)$, reformulate the ODEs as rescaled Picard integral equations over the time interval $[-1, 1]$. Expand the solution of the integral equations with a Chebyshev series expansion in time. Derive an equivalent zero finding problem of the form $F(a) = 0$ (where $a = (a_{k,j})_{k,j}$ is an infinite two-index sequence of Fourier-Chebyshev coefficients) whose solution correspond to the solution of the Cauchy problem (1). The operator F is defined on the ν -weighed ℓ^1 Banach space $X_{\nu,1}$ of Fourier-Chebyshev coefficients

$$X_{\nu,1} \stackrel{\text{def}}{=} \{a = (a_{k,j})_{k,j} : \|a\|_{X_{\nu,1}} \stackrel{\text{def}}{=} \sum_{k,j} |a_{k,j}| \omega_{k,j} < \infty\}.$$

The weights $\omega_{k,j}$ in the definition of the norm $\|\cdot\|_{X_{\nu,1}}$ are chosen so that (a) they have geometric growth in k (ensuring analyticity of the solutions in space, see Section 2.3); and (b) $X_{\nu,1}$ is a Banach algebra under discrete convolutions of two-index Fourier-Chebyshev sequences. Next, let $\mathcal{L} \stackrel{\text{def}}{=} DF(0)$ be the Fréchet derivative of F at $0 \in X_{\nu,1}$ and use assumption (2) to prove that \mathcal{L} is a boundedly invertible operator on $X_{\nu,1}$ (see Section 3). Then prove that the operator $\mathcal{T}(a) \stackrel{\text{def}}{=} a - \mathcal{L}^{-1}F(a)$ is a contraction on a closed ball $\overline{B_r(\bar{a})}$ of radius $r > 0$ centered at a numerical approximation $\bar{a} \in X_{\nu,1}$. To obtain a proof that the operator $\mathcal{T} : \overline{B_r(\bar{a})} \rightarrow \overline{B_r(\bar{a})}$ is a contraction for some explicit $r > 0$, use a Newton-Kantorovich type theorem (Theorem 2.2) (combining functional analytic estimates and interval arithmetic computations) and the fact that the *step size* $h > 0$ can be taken small if necessary. An application of the contraction mapping theorem yields a unique solution $\tilde{a} \in \overline{B_r(\bar{a})}$ of $F = 0$, which represents the solution of the Cauchy problem on the time interval $[0, h]$. The explicit radius $r > 0$ yields a rigorous C^0 error bound between the true solution of the Cauchy problem (1) and its numerical approximation (see Section 2.3).

To a large extent, the main challenge of this approach is theoretical: show that the operator \mathcal{L} is boundedly invertible on the Banach space $X_{\nu,1}$ and obtain explicit and computable bounds for the operator norm $\|\mathcal{L}^{-1}\|_{B(X_{\nu,1})}$. As described in Section 2, the operator $\mathcal{L} = (\mathcal{L}_k)_k$ is a block diagonal operator, where each block \mathcal{L}_k acts on the sequence of Chebyshev coefficients of the Fourier mode $a_k(t)$, and consists of the sum of an infinite-dimensional tridiagonal operator and a rank one operator. To show that \mathcal{L} is a boundedly invertible operator, we show that each block \mathcal{L}_k is boundedly invertible on the ℓ^1 Banach space of Chebyshev sequences. For a finite number of blocks \mathcal{L}_k with k small, we use that \mathcal{L}_k is diagonal dominant starting from a moderately low Chebyshev dimension $N(k)$ to construct (with computer-assistance) an explicit approximate inverse A_k for \mathcal{L}_k (see Figure 1) which is then used in a Neumann series argument to get a rigorous bound

on $\|\mathcal{L}_k^{-1}\|_{B(\ell^1)}$ (see Lemma 3.1). As the Fourier dimension, k grows, the Chebyshev projection number $N(k)$ from which the operator \mathcal{L}_k is diagonal dominant goes to infinity, and therefore the approach for small k is not readily applicable. Hence, we derive an alternative and analytic approach to obtain a uniform bound $\|\mathcal{L}_k^{-1}\|_{B(\ell^1)}$ for large k (see Section 3). The approach here is also computer-assisted, utilizing both the numerical (C++) and symbolic (Mathematica) computation. It is based on the explicit inverse tri-diagonal operator analytic formulas introduced in [20]. Combining the computer-assisted technique for small k and the one for large k , we obtain a rigorous bound for $\|\mathcal{L}^{-1}\|_{B(X_{\nu,1})}$. We remark that forfeiting the diagonal dominance of \mathcal{L}_k for large k has been the main obstacle in deriving a forward integration scheme for parabolic PDE via the Chebyshev series. To the best of our knowledge, we present a first successful purely spectral approach for forward integration of parabolic PDEs via Chebyshev series (this is in contrast with the approach [11, 12] which also uses Chebyshev series expansions in time but handles the contraction mapping theorem via the semi-group flow action). Moreover, we believe that our technique of constructing explicit norm bounds of \mathcal{L}_k operator for large k is of independent interest.

The novelty of our approach is threefold. First, it introduces a computational framework to handle infinite-dimensional problems with operators having the property that the non-diagonal tri-diagonal entries of \mathcal{L}_k are unbounded as k grows (in contrast, the approach of [21] handles problems with tri-diagonal operators having unbounded off-diagonal entries, but the operators are still diagonal dominant). Second, once the bound on $\|\mathcal{L}^{-1}\|_{B(X_{\nu,1})}$ is obtained, the approach is rather straightforward to implement, computationally inexpensive and readily applicable to different models satisfying assumption (2). We stress that simple and efficient implementation is highly desired from the perspective of verifying code correctness of computer-assisted proofs in dynamics, namely clean and verifiable implementation is more likely to be widely accepted by the community. Third, contrary to time-stepping schemes, like the forward integration method based on the Taylor expansion and the Lohner algorithm from [2, 3], extended in [4], our approach is not burdened with the stiffness issue coming from the appearance of large positive and negative eigenvalues of the linear operator spectrum. The approximation quality yielded by the Chebyshev series expansion allows stable and high accuracy numerics (see the applications in Section 5, where the considered examples have many (sometimes large) unstable eigenvalues). We believe that our approach will eventually make possible time-integration for PDE parameter regimes that have not been treated so far.

We must nevertheless confess that our approach has some limitations. The most important one is that assumption (2) is restrictive (e.g. our approach does not apply to Burgers' equation, the Cahn-Hilliard equation, or the Ohta-Kawasaki model) and that we do not foresee for the moment a way to overcome this theoretical limitation. There are two less worrisome limitations: (a) in the current setting, large step sizes h are only possible when the norm of the solution is small (see Remark 4.5); and (b) there is a rapid propagation of wrapping effect from one step to the next, which prevents our approach to be applied iteratively for a large number of steps (see Remark 4.1). While we do not foresee how to get rid of assumption (2), we strongly believe that the step size restriction and the wrapping effect limitation can be overcome by extending our method even further. This is the subject of future investigation, and we are convinced that further research will lead to the successful elimination of the mentioned limitations. The goal of the present paper is to propose an alternative technique for forward integration of parabolic PDEs, which has not yet been explored and is based on novel principles. A simple implementation of the presented technique already demonstrated interesting experimental results and should lead to a new line of research in computer-assisted proofs in dynamics.

The paper is organized as follows. In Section 2, we derive the zero finding problem $F(a) = 0$ whose solution corresponds to the solution of the Cauchy problem and we introduce a Newton-Kantorovich type argument to compute rigorously solutions to $F = 0$. We demonstrate that the space-time regularity of the solution follows from the proof and that the solution so-obtained is classical (strong). In Section 3, we introduce a technique to show that \mathcal{L} is boundedly invertible on $X_{\nu,1}$ and we obtain explicit and computable bounds for the operator norm $\|\mathcal{L}^{-1}\|_{B(X_{\nu,1})}$. The computer-assisted method to obtain a rigorous bound on $\|\mathcal{L}_k^{-1}\|_{B(\ell^1)}$ for small k is presented in Section 3.1, while in Section 3.2, we introduce the analytic approach

to obtain a uniform bound $\|\mathcal{L}_k^{-1}\|_{B(\ell^1)}$ for large k . In Section 4, we present the construction of the necessary bounds to apply the Newton-Kantorovich type argument. In Section 5, we apply our approach to four well-known PDE models namely Fisher's equation, the Kuramoto-Sivashinsky equation, the Swift-Hohenberg equation, and the phase-field crystal equation. We conclude the paper by discussing future directions.

2 General set-up and a Newton-Kantorovich type argument

This section begins in Section 2.1, where the derivation of the zero finding problem $F(a) = 0$ is presented. The Banach space $X_{\nu,1}$ and some of its properties are introduced, and an equivalent fixed point formulation of the problem is presented. In Section 2.2 we present a Newton-Kantorovich type argument (see Theorem 2.2) which we use to solve $F = 0$. We end in Section 2.3 by showing that the solution obtained from the fixed point argument is classical (strong), and by showing how to get a rigorous C^0 error bound between the exact solution and the numerical approximation of the Cauchy problem.

2.1 The problem formulations and the Banach space

Consider the general PDE (1) and assume it satisfies the assumption (2). We supplement the model with odd (i.e. $u(t, -x) = -u(t, x)$) or even (i.e. $u(t, -x) = u(t, x)$) boundary conditions, in which case we expand solutions using a sine Fourier series

$$u(t, x) = -2 \sum_{k \geq 1} \tilde{a}_k(t) \sin(kx) = \sum_{k \in \mathbb{Z}} i \tilde{a}_k(t) e^{ikx}, \quad \text{with } \tilde{a}_{-k}(t) = -\tilde{a}_k(t) \text{ and } \tilde{a}_0 \equiv 0, \quad (3)$$

or a cosine Fourier series

$$u(t, x) = \tilde{a}_0(t) + 2 \sum_{k \geq 1} \tilde{a}_k(t) \cos(kx) = \sum_{k \in \mathbb{Z}} \tilde{a}_k(t) e^{ikx}, \quad \text{with } \tilde{a}_{-k}(t) = \tilde{a}_k(t). \quad (4)$$

After plugging a Fourier series in (1) (sine or cosine) the model reduces to the infinite system of ordinary differential equations

$$\frac{d\tilde{a}_k}{dt} = f_k(\tilde{a}) = \lambda_k \tilde{a}_k + k^n N_k(\tilde{a}), \quad \text{for all } k \geq k_0 \quad (5)$$

where typically $k_0 \in \{0, 1\}$, where λ_k are the eigenvalues of the linear operator L and where the term $k^n N_k$ corresponds to the action in Fourier space of the nonlinear operator $\partial_x^n N$ of (1). By assumption, the semi-linear PDE model (1) is dissipative, and therefore $\lim_{k \rightarrow \infty} \operatorname{Re}(\lambda_k) = -\infty$.

In this paper, we propose to compute solutions of the Cauchy problem associated to (1) on a given time interval $[0, h]$, where $h > 0$. This naturally leads to study the initial value problem

$$\frac{d}{dt} \tilde{a}_k(t) = f_k(\tilde{a}(t)), \quad \text{for } t \in [0, h] \text{ and } \tilde{a}_k(0) = b_k \text{ for all } k \geq k_0, \quad (6)$$

where the vector $b = (b_k)_k$ corresponds to the Fourier coefficients of the initial condition $u_0(x) = u(0, x)$. We rescale time by the factor $h > 0$ to map the interval $[0, h]$ to $[-1, 1]$ (letting $\tau \stackrel{\text{def}}{=} 2t/h - 1$) so that

$$\frac{d}{d\tau} a_k(\tau) = \frac{h}{2} f_k(a(\tau)), \quad \text{for } \tau \in [-1, 1] \text{ and } a_k(-1) = b_k \text{ for all } k \geq k_0. \quad (7)$$

Rewriting the system (7) as an integral equation results in

$$a_k(\tau) = b_k + \frac{h}{2} \int_{-1}^{\tau} f_k(a(s)) \, ds, \quad k \geq k_0, \quad \tau \in [-1, 1]. \quad (8)$$

For each k , we expand $a_k(\tau)$ using a Chebyshev series, that is

$$a_k(\tau) = a_{k,0} + 2 \sum_{j \geq 1} a_{k,j} T_j(\tau) = a_{k,0} + 2 \sum_{j \geq 1} a_{k,j} \cos(j\theta) = \sum_{j \in \mathbb{Z}} a_{k,j} e^{ij\theta}, \quad (9)$$

where $a_{k,-j} = a_{k,j}$ and $\tau = \cos(\theta)$. The cosine Fourier expansion (4) becomes

$$u(\tau, x) = \sum_{k,j \in \mathbb{Z}} a_{k,j} e^{ij\theta} e^{ikx}, \quad a_{k,-j} = a_{k,j} \text{ and } a_{-k,j} = a_{k,j}, \quad (10)$$

while the sine Fourier expansion (3) becomes

$$u(\tau, x) = \sum_{k,j \in \mathbb{Z}} i a_{k,j} e^{ij\theta} e^{ikx}, \quad a_{k,-j} = a_{k,j} \text{ and } a_{-k,j} = -a_{k,j}. \quad (11)$$

For each $k \geq k_0$, we expand $f_k(a(\tau))$ using a Chebyshev series, that is

$$f_k(a(\tau)) = \phi_{k,0}(a) + 2 \sum_{j \geq 1} \phi_{k,j}(a) \cos(j\theta) = \sum_{j \in \mathbb{Z}} \phi_{k,j}(a) e^{ij\theta}, \quad (12)$$

where

$$\phi_{k,j}(a) = \lambda_k a_{k,j} + k^n N_{k,j}(a).$$

Letting $N_k(a) \stackrel{\text{def}}{=} (N_{k,j}(a))_{j \geq 0}$, $\phi_k(a) \stackrel{\text{def}}{=} (\phi_{k,j}(a))_{j \geq 0}$ and noting that $(\lambda_k a_k)_j = \lambda_k a_{k,j}$, we get that

$$\phi_k(a) = \lambda_k a_k + k^n N_k(a). \quad (13)$$

Combining (8), (9) and (12) leads to

$$\sum_{j \in \mathbb{Z}} a_{k,j} e^{ij\theta} = a_k(\tau) = b_k + \frac{h}{2} \int_{-1}^{\tau} f_k(a(s)) \, ds = b_k + \frac{h}{2} \int_{-1}^{\tau} \sum_{j \in \mathbb{Z}} \phi_{k,j}(a) e^{ij\theta} \, ds$$

and this results (e.g. see in [22]) in solving $\tilde{F} = 0$, where $\tilde{F} = (\tilde{F}_{k,j})_{k,j}$ is given component-wise by

$$\tilde{F}_{k,j}(a) = \begin{cases} a_{k,0} + 2 \sum_{\ell=1}^{\infty} (-1)^\ell a_{k,\ell} - b_k, & j = 0, k \geq k_0 \\ 2ja_{k,j} + \frac{h}{2}(\phi_{k,j+1}(a) - \phi_{k,j-1}(a)), & j > 0, k \geq k_0. \end{cases}$$

Let

$$\tilde{n} \stackrel{\text{def}}{=} \frac{d}{3} - n. \quad (14)$$

Hence, for $j > 0$ and $k \geq k_0$, we aim at solving

$$\tilde{F}_{k,j}(a) = 2ja_{k,j} + \frac{h}{2}\lambda_k(a_{k,j+1} - a_{k,j-1}) + \frac{h}{2}k^n(N_{k,j+1}(a) - N_{k,j-1}(a)) = 0,$$

which is equivalent to solve $F_{k,j}(a) = 0$, where

$$\begin{aligned} F_{k,j}(a) &\stackrel{\text{def}}{=} \frac{2j}{\tilde{k}^{n+\tilde{n}}} a_{k,j} + \frac{h\lambda_k}{2\tilde{k}^{n+\tilde{n}}}(a_{k,j+1} - a_{k,j-1}) + \frac{hk^n}{2\tilde{k}^{n+\tilde{n}}}(N_{k,j+1}(a) - N_{k,j-1}(a)) \\ &= \frac{2j}{\tilde{k}^{d/3}} a_{k,j} + \frac{h\lambda_k}{2\tilde{k}^{d/3}}(a_{k,j+1} - a_{k,j-1}) + \frac{hk^n}{2\tilde{k}^{n+\tilde{n}}}(N_{k,j+1}(a) - N_{k,j-1}(a)), \end{aligned}$$

where $\tilde{k} = 1$, if $k = 0$ and $\tilde{k} = k$ if $k \neq 0$.

To simplify the presentation, we make the assumption that if $n = 0$, then $k_0 = 0$, and if $n > 0$, then $k_0 > 0$. Remark that for all the PDEs considered in the present paper (see Section 5), this hypothesis holds. In this case, this implies that

$$\frac{k^n}{\tilde{k}^{n+\tilde{n}}} = \frac{1}{\tilde{k}^{\tilde{n}}}, \quad \text{for } k \geq k_0.$$

Finally, the problem that we solve is $F = 0$, where $F = (F_{k,j})_{k,j}$ is given component-wise by

$$F_{k,j}(a) \stackrel{\text{def}}{=} \begin{cases} a_{k,0} + 2 \sum_{\ell=1}^{\infty} (-1)^\ell a_{k,\ell} - b_k, & j = 0, k \geq k_0 \\ -\frac{h\lambda_k}{2\tilde{k}^{d/3}} a_{k,j-1} + \frac{2j}{\tilde{k}^{d/3}} a_{k,j} + \frac{h\lambda_k}{2\tilde{k}^{d/3}} a_{k,j+1} + \frac{h}{2\tilde{k}^{\tilde{n}}} (N_{k,j+1}(a) - N_{k,j-1}(a)), & j > 0, k \geq k_0. \end{cases} \quad (15)$$

Define the linear operator \mathcal{L} by

$$\mathcal{L}_{k,j}(a) \stackrel{\text{def}}{=} \begin{cases} a_{k,0} + 2 \sum_{\ell=1}^{\infty} (-1)^\ell a_{k,\ell}, & j = 0, k \geq k_0 \\ \frac{\mu_k}{\tilde{k}^{d/3}} a_{k,j-1} + \frac{2j}{\tilde{k}^{d/3}} a_{k,j} - \frac{\mu_k}{\tilde{k}^{d/3}} a_{k,j+1}, & j > 0, k \geq k_0, \end{cases} \quad (16)$$

where

$$\mu_k \stackrel{\text{def}}{=} -\frac{h}{2} \lambda_k. \quad (17)$$

Note that $\lim_{k \rightarrow \infty} \mu_k = \infty$, and that $\mu_k > 0$ except perhaps for a finite number of indices k . For a fixed Fourier component $k \geq k_0$, the operator \mathcal{L}_k acts on $a_k \stackrel{\text{def}}{=} (a_{k,j})_{j \geq 0}$ and can be visualized as

$$\mathcal{L}_k \stackrel{\text{def}}{=} \begin{pmatrix} 1 & -2 & 2 & -2 & 2 & \cdots \\ \frac{\mu_k}{\tilde{k}^{d/3}} & \frac{2}{\tilde{k}^{d/3}} & -\frac{\mu_k}{\tilde{k}^{d/3}} & 0 & \cdots & \\ 0 & \frac{\mu_k}{\tilde{k}^{d/3}} & \frac{4}{\tilde{k}^{d/3}} & -\frac{\mu_k}{\tilde{k}^{d/3}} & 0 & \cdots \\ \ddots & \ddots & \ddots & \ddots & \ddots & \ddots \\ \cdots & 0 & \frac{\mu_k}{\tilde{k}^{d/3}} & \frac{2j}{\tilde{k}^{d/3}} & -\frac{\mu_k}{\tilde{k}^{d/3}} & \\ & \cdots & \ddots & \ddots & \ddots & \end{pmatrix}. \quad (18)$$

Define the nonlinear operator \mathcal{N} by

$$\mathcal{N}_{k,j}(a) \stackrel{\text{def}}{=} \begin{cases} -b_k, & j = 0, k \geq k_0 \\ \frac{h}{2\tilde{k}^{\tilde{n}}} (N_{k,j+1}(a) - N_{k,j-1}(a)), & j > 0, k \geq k_0. \end{cases} \quad (19)$$

Setting

$$\Lambda \stackrel{\text{def}}{=} \begin{pmatrix} 0 & 0 & 0 & 0 & 0 & \cdots \\ -1 & 0 & 1 & 0 & \cdots & \\ 0 & -1 & 0 & 1 & 0 & \cdots \\ \ddots & \ddots & \ddots & \ddots & \ddots & \ddots \\ \cdots & 0 & -1 & 0 & 1 & \\ & \cdots & \ddots & \ddots & \ddots & \ddots \end{pmatrix}, \quad (20)$$

we may write more densely the nonlinear part \mathcal{N}_k as

$$\mathcal{N}_k(a) = -b_k + \frac{h}{2\tilde{k}^{\tilde{n}}}\Lambda N_k(a), \quad N_k(a) \stackrel{\text{def}}{=} (N_{k,j}(a))_{j \geq 0}.$$

Given a fixed Fourier mode $k \geq k_0$, the formulation for F in (15) may be more densely written as

$$\begin{aligned} F_k(a) &= \mathcal{L}_k a_k + \mathcal{N}_k(a) \\ &= \mathcal{L}_k a_k - b_k + \frac{h}{2\tilde{k}^{\tilde{n}}}\Lambda N_k(a), \end{aligned}$$

where $F_k(a) \stackrel{\text{def}}{=} (F_{k,j}(a))_{j \geq 0}$. Finding a such that $F_k(a) = 0$ is equivalent (provided that the operator \mathcal{L}_k is boundedly invertible) to find a solution (fixed point) of

$$\mathcal{T}_k(a) \stackrel{\text{def}}{=} \mathcal{L}_k^{-1} \left(b_k - \frac{h}{2\tilde{k}^{\tilde{n}}}\Lambda N_k(a) \right) = a_k, \quad \text{for all } k \geq k_0.$$

Let us introduce the three block diagonal operators

$$\mathcal{L} \stackrel{\text{def}}{=} \begin{pmatrix} \mathcal{L}_{k_0} & 0 & \dots & 0 \\ 0 & \ddots & 0 & \dots \\ \ddots & \ddots & \mathcal{L}_k & \dots \\ 0 & \dots & 0 & \ddots \end{pmatrix}, \quad \mathbf{K}^{-\tilde{n}} \stackrel{\text{def}}{=} \begin{pmatrix} \text{Id} & 0 & 0 & \dots \\ 0 & \ddots & 0 & \dots \\ \ddots & \ddots & \frac{1}{k^{\tilde{n}}}\text{Id} & \dots \\ \dots & 0 & 0 & \ddots \end{pmatrix}, \quad \Lambda \stackrel{\text{def}}{=} \begin{pmatrix} \Lambda & 0 & 0 & \dots \\ 0 & \ddots & 0 & \dots \\ \ddots & \ddots & \Lambda & \dots \\ \dots & 0 & 0 & \ddots \end{pmatrix}. \quad (21)$$

Given $k \geq k_0$, denote $a_k = (a_{k,j})_{j \geq 0}$. Denote $a = (a_{k_0}, \dots, a_k, \dots)$. We obtain

$$\mathcal{L}a = \begin{pmatrix} \mathcal{L}_{k_0} & 0 & \dots & 0 \\ 0 & \ddots & 0 & \dots \\ \ddots & \ddots & \mathcal{L}_k & \dots \\ 0 & \dots & 0 & \ddots \end{pmatrix} \begin{pmatrix} a_{k_0} \\ \vdots \\ a_k \\ \vdots \end{pmatrix} = \begin{pmatrix} \mathcal{L}_{k_0}a_{k_0} \\ \vdots \\ \mathcal{L}_k a_k \\ \vdots \end{pmatrix}, \quad \mathbf{K}^{-\tilde{n}}a = \begin{pmatrix} \frac{1}{k_0^{\tilde{n}}}a_{k_0} \\ \vdots \\ \frac{1}{k^{\tilde{n}}}a_k \\ \vdots \end{pmatrix} \quad \text{and} \quad \Lambda a = \begin{pmatrix} \Lambda a_{k_0} \\ \vdots \\ \Lambda a_k \\ \vdots \end{pmatrix}.$$

We can finally write the map F as

$$F(a) = \mathcal{L}a - b + \frac{h}{2}\mathbf{K}^{-\tilde{n}}\Lambda\mathcal{N}(a), \quad (22)$$

where it is understood that $b_k = (b_{k,j})_{j \geq 0}$ with $b_{k,j} = 0$ for all $j > 0$.

Remark 2.1. As we see in Section 3, the regularity assumption (2) ensures that the operator \mathcal{L} is boundedly invertible on $X_{\nu,1}$ (24), that is $\mathcal{L}^{-1} : X_{\nu,1} \rightarrow X_{\nu,1}$.

If (2) holds, then by Remark 2.1 we may define the fixed point operator as

$$\mathcal{T}(a) \stackrel{\text{def}}{=} a - \mathcal{L}^{-1}F(a) = \mathcal{L}^{-1} \left(b - \frac{h}{2}\mathbf{K}^{-\tilde{n}}\Lambda\mathcal{N}(a) \right). \quad (23)$$

The Banach space in which we look for a fixed point of \mathcal{T} is given by

$$X_{\nu,1} \stackrel{\text{def}}{=} \left\{ a = (a_{k,j})_{\substack{k \geq k_0 \\ j \geq 0}} : \|a\|_{X_{\nu,1}} \stackrel{\text{def}}{=} \sum_{k \geq k_0} \sum_{j \geq 0} |a_{k,j}| \omega_{k,j} < \infty \right\}, \quad (24)$$

where $\nu \geq 1$ and (remember that $k_0 \in \{0, 1\}$)

$$\omega_{k,j} \stackrel{\text{def}}{=} \begin{cases} 1, & k = j = 0 \\ 2, & k = 0, j > 0 \\ 2\nu^k, & k > 0, j = 0 \\ 4\nu^k, & k, j > 0. \end{cases} \quad (25)$$

The choice of the weights (25) is to ensure that $X_{\nu,1}$ is a Banach algebra under discrete convolution, that is

$$\|a * b\|_{X_{\nu,1}} \leq \|a\|_{X_{\nu,1}} \|b\|_{X_{\nu,1}} \quad (26)$$

for all $a, b \in X_{\nu,1}$, where the discrete convolution of a and b is given by

$$(a * b)_{k,j} = \sum_{\substack{k_1+k_2=k \\ j_1+j_2=j \\ k_i, j_i \in \mathbb{Z}}} a_{k_1, j_1} b_{k_2, j_2}, \quad (27)$$

using the symmetries $a_{-k,j} = a_{k,j}$, $b_{-k,j} = b_{k,j}$ for cosine Fourier expansion in space and $a_{-k,j} = -a_{k,j}$, $b_{-k,j} = -b_{k,j}$ for sine Fourier expansion in space.

Denote by ℓ^1 the Banach space

$$\ell^1 \stackrel{\text{def}}{=} \{y = (y_j)_{j \geq 0} : \|y\|_{\ell^1} \stackrel{\text{def}}{=} |y_0| + 2 \sum_{j \geq 1} |y_j| < \infty\}.$$

Denote $\delta_{i,j}$ the Kronecker delta symbol, that is $\delta_{i,j} = 1$ if $i = j$ and 0 otherwise. We can therefore re-write

$$\|a\|_{X_{\nu,1}} = \delta_{k_0,0} \|a_0\|_{\ell^1} + 2 \sum_{k \geq 1} \|a_k\|_{\ell^1} \nu^k, \quad a_k \stackrel{\text{def}}{=} (a_{k,j})_{j \geq 0}.$$

Having presented the problem formulations and the Banach space, we are ready to introduce a Newton-Kantorovich type theorem (sometimes called the radii polynomial approach) to prove the existence of fixed points of \mathcal{T} in $X_{\nu,1}$.

2.2 A Newton-Kantorovich type theorem

Recall the map F given by (22), assume that $\mathcal{L} : X_{\nu,1} \rightarrow X_{\nu,1}$ is boundedly invertible (see Section 3) and recall the fixed point operator \mathcal{T} given in (23). Assume that a numerical approximation \bar{a} such that $\|F(\bar{a})\|_{X_{\nu,1}} \ll 1$ has been computed. Denote by

$$\overline{B_r(\bar{a})} \stackrel{\text{def}}{=} \{a \in X_{\nu,1} : \|a - \bar{a}\|_{X_{\nu,1}} \leq r\}$$

the closed ball of radius $r > 0$ centered in \bar{a} in $X_{\nu,1}$. Denote by $B(X_{\nu,1})$ the space of bounded linear operators on $X_{\nu,1}$ and $\|\cdot\|_{B(X_{\nu,1})}$ the induced operator norm.

Theorem 2.2. *Let Y and $Z = Z(r)$ be bounds satisfying*

$$\|\mathcal{T}(\bar{a}) - \bar{a}\|_{X_{\nu,1}} \leq Y \quad (28)$$

$$\sup_{c \in \overline{B_r(\bar{a})}} \|D_a \mathcal{T}(c)\|_{B(X_{\nu,1})} \leq Z(r). \quad (29)$$

Define the radii polynomial

$$p(r) \stackrel{\text{def}}{=} r(Z(r) - 1) + Y. \quad (30)$$

If there exists $r_0 > 0$ such that

$$p(r_0) < 0,$$

then there exists a unique $\tilde{a} \in \overline{B_{r_0}(\bar{a})}$ satisfying $F(\tilde{a}) = 0$.

Proof. The idea is to show that \mathcal{T} is a contraction mapping of $\overline{B_{r_0}(\bar{a})}$ into itself, in which case the result follows from the contraction mapping theorem.

Let $a \in \overline{B_{r_0}(\bar{a})}$ and apply the Mean Value Inequality to obtain

$$\begin{aligned}\|\mathcal{T}(a) - \bar{a}\|_{X_{\nu,1}} &\leq \|\mathcal{T}(a) - \mathcal{T}(\bar{a})\|_{X_{\nu,1}} + \|\mathcal{T}(\bar{a}) - \bar{a}\|_{X_{\nu,1}} \\ &\leq \sup_{c \in \overline{B_{r_0}(\bar{a})}} \|D_a \mathcal{T}(c)\|_{B(X_{\nu,1})} \|a - \bar{a}\|_{X_{\nu,1}} + Y \\ &\leq r_0 Z(r_0) + Y,\end{aligned}$$

where the last inequality follows from (28) and (29). Using that $p(r_0) < 0$ implies that $\|\mathcal{T}(a) - \bar{a}\|_{X_{\nu,1}} < r_0$ and therefore that $\mathcal{T} : \overline{B_{r_0}(\bar{a})} \rightarrow \overline{B_{r_0}(\bar{a})}$.

To see that \mathcal{T} is a contraction on $\overline{B_{r_0}(\bar{a})}$, let $c_1, c_2 \in \overline{B_{r_0}(\bar{a})}$ and see that

$$\begin{aligned}\|\mathcal{T}(c_1) - \mathcal{T}(c_2)\|_{X_{\nu,1}} &\leq \sup_{c \in \overline{B_{r_0}(\bar{a})}} \|D_a \mathcal{T}(c)\|_{B(X_{\nu,1})} \|c_1 - c_2\|_{X_{\nu,1}} \\ &\leq Z(r_0) \|c_1 - c_2\|_{X_{\nu,1}}.\end{aligned}$$

Again, from the assumption that $p(r_0) < 0$ (that is $r_0 Z(r_0) + Y < r_0$), it follows that

$$Z(r_0) < 1 - \frac{Y}{r_0} \leq 1.$$

Hence $\mathcal{T} : \overline{B_{r_0}(\bar{a})} \rightarrow \overline{B_{r_0}(\bar{a})}$ is a contraction with contraction constant $Z(r_0) < 1$. The contraction mapping theorem yields the existence of a unique $\tilde{a} \in \overline{B_{r_0}(\bar{a})}$ such that $\mathcal{T}(\tilde{a}) = \tilde{a} = \tilde{a} - \mathcal{L}^{-1}F(\tilde{a})$. Since \mathcal{L} is invertible, \mathcal{L}^{-1} is invertible and this implies that \tilde{a} is the unique element of $\overline{B_{r_0}(\bar{a})}$ satisfying $F(\tilde{a}) = 0$. \square

In Section 4, we construct explicitly the bounds necessary to apply the (radii polynomial) approach of Theorem 2.2.

We conclude this section by introducing two consequences of a successful application of Theorem 2.2. The first one is that we get enough space and time regularity of the solution so that we obtain a classical solution to the Cauchy problem. The second one is that the radius $r_0 > 0$ such that $p(r_0) < 0$ provides in fact a rigorous C^0 error control between the exact solution and a numerical approximation of the Cauchy problem.

2.3 Regularity of the solutions and rigorous C^0 error control

Assume that we applied the (radii polynomial) approach of Theorem 2.2 to prove the existence of $\tilde{a} \in X_{\nu,1}$ such that $F(\tilde{a}) = 0$ and $\|\tilde{a} - \bar{a}\|_{X_{\nu,1}} \leq r_0$ where F is defined in (22), $\nu \geq 1$ and \bar{a} is a numerical approximation. This is done by verifying that $r_0 > 0$ satisfies $p(r_0) < 0$. Denote by

$$\tilde{u}(\tau, x) \stackrel{\text{def}}{=} \begin{cases} \sum_{k,j \in \mathbb{Z}} \tilde{a}_{k,j} e^{ijk\theta} e^{ikx}, & \tilde{a}_{k,-j} = \tilde{a}_{k,j} \text{ and } \tilde{a}_{-k,j} = \tilde{a}_{k,j}, \quad \tilde{u} \text{ even} \\ \sum_{k,j \in \mathbb{Z}} i\tilde{a}_{k,j} e^{ijk\theta} e^{ikx}, & \tilde{a}_{k,-j} = \tilde{a}_{k,j} \text{ and } \tilde{a}_{-k,j} = -\tilde{a}_{k,j}, \quad \tilde{u} \text{ odd} \end{cases} \quad (31)$$

the corresponding Fourier-Chebyshev expansion.

If $\nu > 1$, then for each $k > 0$, $2\|\tilde{a}_k\|_{\ell^1} \nu^k \leq \delta_{k_0,0} \|\tilde{a}_0\|_{\ell^1} + 2 \sum_{k \geq 1} \|\tilde{a}_k\|_{\ell^1} \nu^k = \|\tilde{a}\|_{X_{\nu,1}} < \infty$, and therefore

$$\|\tilde{a}_k\|_{\ell^1} \leq \frac{\|\tilde{a}\|_{X_{\nu,1}}}{2\nu^k}, \quad \text{for all } k > 0,$$

which has a geometric decay rate. Hence, we get the analyticity of the solutions in space and the \tilde{u} has enough classical derivatives in space to be evaluated in the PDE model (1). If $\nu = 1$, then by continuity of the bounds Y and $Z(r)$ in the decay rate ν , there exists $\epsilon > 0$ such that $p(r) < 0$ for some $\tilde{\nu} = 1 + \epsilon > 1$, and therefore we are back to the previous case and space regularity follows (for a similar and more detailed argument, see Proposition 3 in [23]). As for the time regularity, it follows from the fact that for each k , $\tilde{a}_k(\tau)$ is continuous in τ and solves the Picard integral equation (8). By continuity of f_k , $f_k(\tilde{a}(\tau))$ is continuous and therefore $\int_{-1}^{\tau} f_k(a(s)) ds$ is differentiable and therefore \tilde{a}_k is differentiable in time. This follows that the resulting Fourier-Chebyshev expansion $\tilde{u}(\tau, x)$ given in (31) is a classical (strong) solution of (1).

Finally, denote by

$$\bar{u}(\tau, x) \stackrel{\text{def}}{=} \begin{cases} \sum_{k,j \in \mathbb{Z}} \bar{a}_{k,j} e^{ij\theta} e^{ikx}, & \bar{a}_{k,-j} = \bar{a}_{k,j} \text{ and } \bar{a}_{-k,j} = \tilde{a}_{k,j}, \quad \bar{u} \text{ even} \\ \sum_{k,j \in \mathbb{Z}} i\bar{a}_{k,j} e^{ij\theta} e^{ikx}, & \bar{a}_{k,-j} = \bar{a}_{k,j} \text{ and } \bar{a}_{-k,j} = -\bar{a}_{k,j}, \quad \bar{u} \text{ odd} \end{cases}$$

the corresponding numerical approximate Fourier-Chebyshev expansion of the Cauchy problem. Then,

$$\begin{aligned} \|\tilde{u} - \bar{u}\|_{C^0} &\stackrel{\text{def}}{=} \sup_{\substack{\tau \in [-1, 1] \\ x \in [0, 2\pi]}} |\tilde{u}(\tau, x) - \bar{u}(\tau, x)| \\ &\leq \sum_{k,j \in \mathbb{Z}} |\tilde{a}_{k,j} - \bar{a}_{k,j}| |e^{ij\theta} e^{ikx}| \\ &\leq \sum_{k \geq k_0} \sum_{j \geq 0} |\tilde{a}_{k,j} - \bar{a}_{k,j}| \omega_{k,j} \\ &= \|\tilde{a} - \bar{a}\|_{X_{\nu,1}} \leq r_0. \end{aligned} \tag{32}$$

This shows that the radius $r_0 > 0$ such that $p(r_0) < 0$ (from the radii polynomial approach) provides in fact a rigorous C^0 error control between the exact solution \tilde{u} and the numerical approximation \bar{u} of the Cauchy problem.

We are now ready to introduce the theory to show that \mathcal{L} is boundedly invertible, to obtain rigorous estimates on $\|\mathcal{L}_k^{-1}\|_{B(\ell^1)}$ for all $k \geq k_0$ and finally to derive an explicit and computable bound for $\|\mathcal{L}^{-1}\|_{B(X_{\nu,1})}$.

3 Analysis of the linear operator \mathcal{L}

In this section, we introduce our approach to prove that the operator \mathcal{L} is boundedly invertible on $X_{\nu,1}$ and we obtain explicit and computable bounds for the operator norm $\|\mathcal{L}^{-1}\|_{B(X_{\nu,1})}$. In Section 3.1, we consider small k and use that \mathcal{L}_k is diagonal dominant starting from a moderately low Chebyshev dimension $N(k)$ to construct (with computer-assistance) an explicit approximate inverse. The approximate inverse is used in a Neumann series argument to obtain a rigorous bound on $\|\mathcal{L}_k^{-1}\|_{B(\ell^1)}$. Then in Section 3.2, we introduce an approach to obtain a uniform bound $\|\mathcal{L}_k^{-1}\|_{B(\ell^1)}$ for large k . The approach here is also computer-assisted, utilizing both the numerical and symbolic computation. It is based on the explicit inverse tri-diagonal operator analytic formulas introduced in [20]. Combining the computer-assisted technique for small k and the one for large k , we introduce in Section 3.3 a bound for $\|\mathcal{L}^{-1}\|_{B(X_{\nu,1})}$.

3.1 Bounds for $\|\mathcal{L}_k^{-1}\|_{B(\ell^1)}$ for small k

We begin this section by introducing some operators. Fix a number N , and denote the operators $\tilde{\Lambda}$ and Ω acting on the tail of a Chebyshev sequence as

$$\tilde{\Lambda} \stackrel{\text{def}}{=} \begin{pmatrix} 0 & -1 & 0 & \cdots & & \\ 1 & 0 & -1 & 0 & \cdots & \\ 0 & 1 & 0 & -1 & \cdots & \\ \ddots & \ddots & \ddots & \ddots & \ddots & \\ \cdots & 0 & 1 & 0 & -1 & \\ & \cdots & \ddots & \ddots & \ddots & \end{pmatrix} \quad \text{and} \quad \Omega \stackrel{\text{def}}{=} \begin{pmatrix} 2N & 0 & 0 & \cdots & & \\ 0 & 2(N+1) & 0 & 0 & & \\ 0 & 0 & 2(N+2) & 0 & & \\ \vdots & \vdots & \ddots & \ddots & \ddots & \\ & & & & \ddots & \ddots \end{pmatrix}.$$

Fix $k \geq k_0$ and let

$$\tilde{\mu}_k \stackrel{\text{def}}{=} \frac{\mu_k}{\tilde{k}^{d/3}} = -\frac{h\lambda_k}{2\tilde{k}^{d/3}}.$$

Using $\tilde{\mu}_k$ and the above *tail* operators, rewrite the operator \mathcal{L}_k in (18) as in Figure 1, where $M \in M_N(\mathbb{R})$ is the matrix consisting of the first $N \times N$ entries of \mathcal{L}_k . Denote the infinite dimensional row vector $v \stackrel{\text{def}}{=} (-2 \ 2 \ -2 \ 2 \ -2 \ 2 \ \cdots)$, which is the tail of the first row of the operator \mathcal{L}_k . Define the operator A_k (which acts as an approximate inverse for \mathcal{L}_k) as given in Figure 1.

$$\mathcal{L}_k = \left[\begin{array}{c|c} M & \begin{smallmatrix} -2 & 2 & -2 & 2 & -2 & 2 & \cdots \\ \hline & 0 & & & & & \end{smallmatrix} \\ \hline 0 & \begin{smallmatrix} \tilde{\mu}_k \\ \hline \frac{1}{\tilde{k}^{d/3}} \Omega + \tilde{\mu}_k \tilde{\Lambda} \end{smallmatrix} \end{array} \right] \quad \text{and} \quad A_k = \left[\begin{array}{c|c} M^{-1} & \begin{smallmatrix} -\tilde{k}^{d/3} M_{col(1)}^{-1} v \Omega^{-1} \\ \hline & 0 & & & & & \end{smallmatrix} \\ \hline 0 & \begin{smallmatrix} \tilde{k}^{d/3} \Omega^{-1} \end{smallmatrix} \end{array} \right]$$

Figure 1: The operator \mathcal{L}_k and its approximate inverse operator A_k .

Lemma 3.1. *Let $N \in \mathbb{N}$. Assume that $M \in M_N(\mathbb{R})$ is invertible, and consider the operator \mathcal{L}_k as in Figure 1. Let*

$$\rho^{(1)} \stackrel{\text{def}}{=} \frac{1}{N} \left(\|M_{col(1)}^{-1}\|_{\ell^1} + \frac{1}{2} \right) \quad (33)$$

$$\rho^{(2)} \stackrel{\text{def}}{=} \left\| \frac{1}{\tilde{k}^{d/3}} M_{col(N)}^{-1} + \frac{1}{N+1} M_{col(1)}^{-1} \right\|_{\ell^1} + \frac{1}{2(N+1)} \quad (34)$$

$$\rho^{(3)} \stackrel{\text{def}}{=} \frac{2}{N(N+2)} \|M_{col(1)}^{-1}\|_{\ell^1} + \frac{1}{2N} + \frac{1}{2(N+2)} \quad (35)$$

and

$$\rho_k \stackrel{\text{def}}{=} |\mu_k| \max\{\rho^{(1)}, \rho^{(2)}, \rho^{(3)}\}, \quad (36)$$

where $M_{col(1)}^{-1} \in \mathbb{R}^N$ denotes the first column of the matrix M^{-1} . Let

$$\beta_k \stackrel{\text{def}}{=} \max \left\{ \|M^{-1}\|_{B(\ell^1)}, \frac{\tilde{k}^{d/3}}{N} \left(\|M_{col(1)}^{-1}\|_{\ell^1} + \frac{1}{2} \right) \right\}. \quad (37)$$

If $\rho_k < 1$, then \mathcal{L}_k is a boundedly invertible operator on ℓ^1 with

$$\|\mathcal{L}_k^{-1}\|_{B(\ell^1)} \leq \frac{\beta_k}{1 - \rho_k}. \quad (38)$$

Proof. From the definition of the operators A_k and \mathcal{L}_k in Figure 1, one can verify that the linear operator $I - A_k \mathcal{L}_k$ is given in Figure 2, where the operator $\widetilde{M}_{col(N)}^{-1}$ is also defined in Figure 2. From this, we get

$$I - A_k \mathcal{L}_k = \mu_k \begin{bmatrix} 0 & \left| \begin{array}{c|c} -\frac{1}{N} M_{col(1)}^{-1} & \frac{1}{\tilde{k}^{\frac{d}{3}}} \widetilde{M}_{col(N)}^{-1} + M_{col(1)}^{-1} v \Omega^{-1} \tilde{\Lambda} \\ \hline & \frac{1}{2N} \end{array} \right| \\ \hline 0 & -\Omega^{-1} \tilde{\Lambda} \end{bmatrix}, \quad \widetilde{M}_{col(N)}^{-1} = \begin{bmatrix} \vdots \\ M_{col(N)}^{-1} \\ \vdots \\ 1 \end{bmatrix} \quad \begin{bmatrix} 0 & \cdots \end{bmatrix}$$

Figure 2: The operators $I - A_k \mathcal{L}_k$ and $\widetilde{M}_{col(N)}^{-1}$.

that the first $N - 1$ columns of $I - A_k \mathcal{L}_k$ are zero. The ℓ^1 norm of the N^{th} column of $I - A_k \mathcal{L}_k$ is given by $|\mu_k| \rho^{(1)}$, where $\rho^{(1)}$ is defined in (33). Let us now compute explicitly the j^{th} columns of $I - A_k \mathcal{L}_k$ for $j > N$. For this, we need to explicitly obtain the j^{th} column of $M_{col(1)}^{-1} v \Omega^{-1} \tilde{\Lambda}$. Let us first look at the *row* vector $v \Omega^{-1} \tilde{\Lambda}$, which is given by

$$v \Omega^{-1} \tilde{\Lambda} = \left(\frac{1}{N+1}, \frac{1}{N} - \frac{1}{N+2}, -\frac{1}{N+1} + \frac{1}{N+3}, \dots, \frac{2(-1)^j}{(N+j-2)(N+j)}, \dots \right),$$

and therefore for $j > N$,

$$\left(M_{col(1)}^{-1} v \Omega^{-1} \tilde{\Lambda} \right)_{col(j)} = \begin{cases} \frac{1}{N+1} M_{col(1)}^{-1}, & j = N+1 \\ \frac{2(-1)^j}{(j-2)j} M_{col(1)}^{-1}, & j \geq N+2. \end{cases} \quad (39)$$

Hence, the finite part of the $(N+1)^{th}$ column of $\frac{1}{\mu_k} (I - A_k \mathcal{L}_k)$ is given by the sum of (a) $\tilde{k}^{-d/3}$ times the first column of the operator $\widetilde{M}_{col(N)}^{-1}$ (see Figure 2), that is $\tilde{k}^{-d/3} M_{col(N)}^{-1}$; and (b) the first column of the operator $M_{col(1)}^{-1} v \Omega^{-1} \tilde{\Lambda}$, that is (using (39)) $\frac{1}{N+1} M_{col(1)}^{-1}$. Moreover, the *tail* part of the $(N+1)^{th}$ column of $\frac{1}{\mu_k} (I - A_k \mathcal{L}_k)$ is given by $(0, -\frac{1}{2(N+1)}, 0, 0, \dots)^T$. We conclude from this analysis that the ℓ^1 norm of the $(N+1)^{th}$ column of $I - A_k \mathcal{L}_k$ is given by $|\mu_k| \rho^{(2)}$, where $\rho^{(2)}$ is defined in (34).

For $j > N+1$, using (39), the finite part of the $(N+1)^{th}$ column of $\frac{1}{\mu_k} (I - A_k \mathcal{L}_k)$ is given by $\frac{2(-1)^j}{(N+j-2)(N+j)} M_{col(1)}^{-1}$ while the tail part is given by $(0, 0, \dots, 0, -\frac{1}{2(j-2)}, 0, \frac{1}{2j}, 0, 0, \dots)^T$. We conclude from this that for $j \geq N+2$, the ℓ^1 norm of the k^{th} column of $I - A_k \mathcal{L}_k$ is given by $|\mu_k| \rho^{(3)}$, where $\rho^{(3)}$ is defined in (35).

Therefore, we get that

$$\|I - A_k \mathcal{L}_k\|_{B(\ell^1)} = \rho_k < 1,$$

by assumption. By a Neumann series argument, $A_k \mathcal{L}_k$ is invertible with

$$(A_k \mathcal{L}_k)^{-1} = \sum_{j \geq 0} (I - A_k \mathcal{L}_k)^j.$$

By construction, A_k is invertible. Hence, \mathcal{L}_k is invertible with

$$\mathcal{L}_k^{-1} = \left(\sum_{j \geq 0} (I - A_k \mathcal{L}_k)^j \right) A_k. \quad (40)$$

Using (37), we conclude the proof realizing that

$$\|\mathcal{L}_k^{-1}\|_{B(\ell^1)} \leq \sum_{j \geq 0} (\|I - A_k \mathcal{L}_k\|_{B(\ell^1)})^j \|A_k\|_{B(\ell^1)} \leq \frac{1}{1 - \rho_k} \|A_k\|_{B(\ell^1)} = \frac{\beta_k}{1 - \rho_k}. \quad \square$$

3.2 Uniform bound for $\|\mathcal{L}_k^{-1}\|_{B(\ell^1)}$ for large k

We derive an uniform bound for $\|\mathcal{L}_k^{-1}\|_{B(\ell^1)}$ for large k , by bounding the norms of finite operator projections (matrices) $P_N \mathcal{L}_k (P_N a)$ with respect to the Galerkin approximation dimension N , where P_N denotes the projection onto N dominating Chebyshev coefficients.

We bound the norms $\|P_N \mathcal{L}_k (P_N a)\|_{B(\ell^1)}$ uniformly with respect to the projection size N , therefore the bound for $\|\mathcal{L}_k^{-1}\|_{B(\ell^1)}$ follows. For the purpose of this section we fix the Galerkin approximation dimension N , and the index k (assuming it is large – made precise in statements of the theorems). We slightly abuse the notation, and use the same notation to denote the projected as well as the full operator.

First, we are concerned with bounding the norm of the inverse of tri-diagonal part of \mathcal{L}_k , excluding the first row and column ($\tilde{k}^{-d/3} \cdot T_k$). Second, using the Sherman-Morrison formula we eventually bound $\|\mathcal{L}_k^{-1}\|_{B(\ell^1)}$ by simply a multiple of the inverse of tri-diagonal part bound.

Notation For a square matrix A by $A_{col(i)}$ we denote the i -th column vector of A , by $A_{row(j)}$ we denote the j -th row vector of A , by $A_{col(i:j)}$ we denote the matrix composed out of the i, \dots, j -th columns of A , by $A_{row(i:j)}$ we denote the matrix composed out of the i, \dots, j -th rows of A .

We like to exploit the tridiagonal form of \mathcal{L}_k , so we decompose \mathcal{L}_k into a sum of a tridiagonal matrix and a rank one matrix, i.e.

$$\mathcal{L}_k = A_k + U = \begin{bmatrix} 1 & 0 & \cdots & 0 \\ \mu_k \tilde{k}^{-d/3} & \tilde{k}^{-d/3} \cdot T_k & & \\ 0 & & & \\ \vdots & & & \end{bmatrix} + \begin{bmatrix} 0 & -2 & 2 & \cdots \\ & & 0 & \\ & & & \end{bmatrix}, \quad (41)$$

where

$$T_k = \begin{bmatrix} 2 & -\mu_k & 0 & \cdots & \cdots \\ \mu_k & 4 & -\mu_k & 0 & \cdots \\ \ddots & \ddots & \ddots & \ddots & \ddots \\ \dots & 0 & \mu_k & 2(N-1) & -\mu_k \\ & \dots & 0 & \mu_k & 2N \end{bmatrix} \quad (42)$$

3.2.1 Finite inverse tridiagonal operator $\|\tilde{k}^{d/3} \cdot T_k^{-1}\|_{B(\ell^1)}$ norm uniform with respect to N

Notation Let $N > 0$ be an even integer defining the projection size (fixed), $k > 1$. Given sequence $\{d_j\}_{j=1}^N$ by

$$T_k(d_1, \dots, d_N) = \begin{bmatrix} d_1 & -\mu_k & 0 & \dots & \dots \\ \mu_k & d_2 & -\mu_k & 0 & \dots \\ \ddots & \ddots & \ddots & \ddots & \ddots \\ \dots & 0 & \mu_k & d_{N-1} & -\mu_k \\ \dots & 0 & \mu_k & d_N & \end{bmatrix}, \quad (43)$$

we denote the $N \times N$ tridiagonal matrix with the sequence on the diagonal, and $\pm\mu_k$ under and over-diagonal respectively.

We assume that k denoting the Fourier coefficient is fixed, and denote $T = T_k$. By default T without parentheses denotes the matrix with the sequence $d_k = 2k$ as its diagonal (3.3), for $k \geq 1$. We also use the notation $T^{-1}(d_1, \dots, d_N)$ to denote the inverse of $T(d_1, \dots, d_N)$. Observe that any matrix having the tridiagonal form like (43) is invertible due to an easy determinant computation (demonstrated in [20]). If not specified otherwise, we assume that $\mu_k > 0$.

Remark 3.2. We base our large tridiagonal matrices analysis on a kind of divide and conquer paradigm, that is, in order to invert a large tridiagonal matrix we decompose it recursively into smaller and smaller blocks. The blocks appearing in the inverse have a simple and explicit form. In Lemma 3.4 we formalize this observation, to which we are going to refer often in the forthcoming analysis. The formulas that we used are essentially a special case of a formula known in the literature as Banachiewicz inversion formula based on Schur complement [24]. The same formula in the context of validated numerical method was used in [25].

The presented analysis was used already in [20], where it is shown that $\|T_k^{-1}\|_{B(\ell^1)}$ is bounded

Theorem 3.3 (Thm. 4.11 in [20], setting $m = 1$). For any $\mu_k \in \mathbb{R}$. For all k and N , $\|T_k^{-1}\|_{B(\ell^1)}$ is bounded by a constant independent of μ .

However, in the present paper we make the results stronger by not only showing that $\|\tilde{k}^{-d/3} \cdot T_k^{-1}\|_{B(\ell^1)}$ is bounded uniformly in k and N , but also derive an explicit upper bound for it. We provide a new theoretical framework building upon the auxiliary lemmas from [20], and eventually prove the main theorem by means of a computer-assisted proof.

Notation Let μ_k denote the $n \times (N - n)$ matrix having single non-zero element in the lower left corner

$$\mu_k = \begin{bmatrix} 0 & & & & 0 \\ \vdots & \ddots & & & \vdots \\ 0 & 0 & & & 0 \\ \mu_k & 0 & \dots & 0 & \end{bmatrix}, \text{ then } \mu_k \mu_k^T = \begin{bmatrix} & & & 0 \\ & \ddots & & \vdots \\ & & 0 & 0 \\ 0 & \dots & 0 & \mu_k^2 \end{bmatrix} \in M_n(\mathbb{R}). \quad (44)$$

Lemma 3.4. Let $0 < n < N$ be even. Let $T \in \mathbb{R}^{N \times N}$ be a tridiagonal matrix of the form (43) with an arbitrary sequence on the diagonal. T is decomposed in the following way

$$T = \begin{bmatrix} F & -\mu_k \\ \mu_k^T & R \end{bmatrix},$$

where $F \in M_n(\mathbb{R})$, and $R \in M_{N-n}(\mathbb{R})$. Then it holds that

$$T^{-1} = \begin{bmatrix} F & -\mu_k \\ \mu_k^T & R \end{bmatrix}^{-1} = \begin{bmatrix} (F + \mu_k \mu_k^T R_{11}^{-1})^{-1} & F^{-1} \mu_k (R + \mu_k^T \mu_k F_{nn}^{-1})^{-1} \\ -R^{-1} \mu_k^T (F + \mu_k \mu_k^T R_{11}^{-1})^{-1} & (R + \mu_k^T \mu_k F_{nn}^{-1})^{-1} \end{bmatrix}.$$

This formula is a special case of a formula known in literature as Banachiewicz inversion formula based on Schur complement [24].

Proof. We want to compute

$$T^{-1} = \begin{bmatrix} \text{Inv}_{11} & \text{Inv}_{12} \\ \text{Inv}_{21} & \text{Inv}_{22} \end{bmatrix},$$

where $\text{Inv}_{11}, \text{Inv}_{12}, \text{Inv}_{21}, \text{Inv}_{22}$ are the blocks composing T^{-1} of appropriate dimensions.

Directly from the condition for the inverse matrix it follows that

$$\begin{aligned} F\text{Inv}_{11} - \mu_k \text{Inv}_{21} &= I, & \mu_k^T \text{Inv}_{11} + R\text{Inv}_{21} &= 0, \\ F\text{Inv}_{12} - \mu_k \text{Inv}_{22} &= 0, & \mu_k^T \text{Inv}_{12} + R\text{Inv}_{22} &= I. \end{aligned}$$

The presented formula for Inv_{ij} can be obtained by noting

$$\mu_k R^{-1} \mu_k^T = \mu_k \mu_k^T (R_{11}^{-1}), \quad \mu_k^T F^{-1} \mu_k = \mu_k^T \mu_k (F_{nn}^{-1}),$$

and decoupling the solutions to the equations for $\text{Inv}_{11}, \text{Inv}_{12}, \text{Inv}_{21}, \text{Inv}_{22}$. \square

Definition 3.5. Let $\{d_j\}_{j=1}^N$ be the sequence of T_k diagonal elements, let us define the following recursive sequences $a_0, \hat{a}_0, b_0 = 0$

$$\begin{aligned} a_j &= T_{11}^{-1}(d_{N-2j+1}, d_{N-2j+2} + a_{j-1} \mu_k^2) = \frac{d_{N-2j+2} + a_{j-1} \mu_k^2}{d_{N-2j+1} d_{N-2j+2} + a_{j-1} d_{N-2j+1} \mu_k^2 + \mu_k^2} \\ \hat{a}_j &= T_{21}^{-1}(d_{N-2j+1}, d_{N-2j+2} + a_{j-1} \mu_k^2) = \frac{\mu_k}{d_{N-2j+1} d_{N-2j+2} + a_{j-1} d_{N-2j+1} \mu_k^2 + \mu_k^2} \\ b_j &= T_{11}^{-1}(d_{2j-1} + b_{j-1} \mu_k^2, d_{2j}) = \frac{d_{2j-1} + b_{j-1} \mu_k^2}{d_{2j} d_{2j-1} + b_{j-1} d_{2j} \mu_k^2 + \mu_k^2} \end{aligned}$$

for $j = 1, 2, 3, \dots, \frac{N}{2}$.

Lemma 3.6. Let $\{a_j\}_{j=1}^{\frac{N}{2}}, \{\hat{a}_j\}_{j=1}^{\frac{N}{2}}, \{b_j\}_{j=1}^{\frac{N}{2}}$ be the recursive sequences defined in Def. 3.5. It holds that

$$a_j(a_{j-1}), b_j(b_{j-1})$$

are increasing for $j = 2, \dots, \frac{N}{2}$. And

$$\hat{a}_j(a_{j-1})$$

is decreasing for $j = 2, \dots, \frac{N}{2}$.

Proof. We treat a_{j-1}, b_{j-1} as (continuous) variables in the formulas given in Def. 3.5, and compute

$$\begin{aligned} \frac{d a_j}{d a_{j-1}} &= \frac{\mu_k^4}{(d_{N-2j+1} d_{N-2j+2} + a_{j-1} d_{N-2j+1} \mu_k^2 + \mu_k^2)^2} \geq 0, \\ \frac{d b_j}{d b_{j-1}} &= \frac{\mu_k^4}{(d_{2j} d_{2j-1} + b_{j-1} d_{2j} \mu_k^2 + \mu_k^2)^2} \geq 0, \\ \frac{d \hat{a}_j}{d a_{j-1}} &\leq 0. \end{aligned}$$

\square

Lemma 3.7. Let $\{a_j\}_{j=1}^{\frac{N}{2}}$, $\{\hat{a}_j\}_{j=1}^{\frac{N}{2}}$, $\{b_j\}_{j=1}^{\frac{N}{2}}$ be the sequences defined in Def. 3.5. It holds that

$$0 < a_j < \frac{\sqrt{2}}{\mu_k}, \quad 0 < \hat{a}_j < \frac{1}{\mu_k}, \quad 0 < b_j < \frac{1}{\mu_k}$$

for all $j = 1, \dots, \frac{N}{2}$.

Proof. The bound $a_j > 0$ is obvious. First, we show that $a_1 = \frac{d_N}{d_{N-1}d_N + \mu_k^2} < \frac{\alpha}{\mu_k}$, which is satisfied for $\alpha \geq 1$, as $0 < \alpha d_{N-1}d_N + \alpha\mu_k^2 - d_N\mu_k$. We proceed by induction, assume that $a_{j-1} < \frac{\alpha}{\mu_k}$, we plug in $a_{j-1} = \frac{\alpha}{\mu_k}$ due to the monotonicity property proved in Lemma 3.6. We verify

$$a_j < \frac{d_{N-2j+2} + \alpha\mu_k}{d_{N-2j+1}d_{N-2j+2} + \alpha d_{N-2j+1}\mu_k + \mu_k^2} < \frac{\alpha}{\mu_k},$$

which is satisfied when $0 < \alpha d_{N-2j+1}d_{N-2j+2} + \mu_k(\alpha^2 d_{N-2j+1} - d_{N-2j+2})$, and

$$0 < \alpha^2 d_{N-2j+1} - d_{N-2j+2} = \alpha^2 2(N-2j+1) - 2(N-2j+2). \quad (45)$$

We analyze the worst case ($j = \frac{N}{2}$), (45) holds for $\alpha \geq \sqrt{2}$. Therefore, the optimal value of α such that $a_j < \frac{\alpha}{\mu_k}$ is $\alpha = \sqrt{2}$. In order to show the second inequality i.e. $\hat{a}_1 = \frac{\mu_k}{d_{N-1}d_N + \mu_k^2} = \frac{\mu_k}{d_{N-1}d_N + \mu_k^2} < \frac{1}{\mu_k}$ for $N > 1$. By induction we show that $0 < \hat{a}_j < \frac{1}{\mu_k}$. Due to the monotonicity property from Lemma 3.6, and the bound Lemma 3.7 we plug in $a_{j-1} = 0$, and obtain

$$0 < \hat{a}_j < \frac{\mu_k}{d_{N-2j+1}d_{N-2j+2} + \mu_k^2} < \frac{1}{\mu_k} \text{ for } N > 1$$

Now let us turn into the third inequality, obviously $b_1 = \frac{d_1}{d_2d_1 + \mu_k^2} < \frac{1}{\mu_k}$. By induction we show that $0 < b_j < \frac{1}{\mu_k}$. Using the monotonicity property from Lemma 3.6 we plug in $b_{\frac{N-2n+2}{2}} = \frac{1}{\mu_k}$ in the formula for $b_{\frac{N-2n}{2}}$ and obtain

$$\frac{d_{N-2n+1} + \mu}{d_{N-2n+1}d_{N-2n+2} + d_{N-2n+2}\mu + \mu^2} < \frac{1}{\mu_k},$$

satisfied if $0 < d_{N-2n+1}d_{N-2n+2} + (d_{N-2n+2} - d_{N-2n+1})\mu$, and clearly for all $n = 1, \dots, \frac{N}{2} - 1$. \square

Lemma 3.8. Let $\{a_j\}_{j=1}^{\frac{N}{2}}$, $\{\hat{a}_j\}_{j=1}^{\frac{N}{2}}$ be the sequences defined in Def. 3.5. Also let $N > 2\mu_k$. It holds that

$$a_j \leq \frac{1}{4\mu_k}, \text{ and } \hat{a}_j \leq \frac{1}{4\mu_k}$$

for all j such that

$$N - 2j + 1 > 2\mu_k \quad \left(j < \frac{N}{2} - \mu_k + 1 \right). \quad (46)$$

Proof. We put $a_{j-1} = \frac{\sqrt{2}}{\mu_k}$ in the formula for a_j , and denote $d_{N-2j+1} = b$, then $d_{N-2j+2} = b + 2$. We verify

$$\frac{b + 2 + \sqrt{2}\mu_k}{b(b + 2) + \sqrt{2}b\mu_k + \mu_k^2} < \frac{1}{4\mu_k},$$

which reduces to

$$b(b + 2) + \sqrt{2}b\mu_k + \mu_k^2 - 4b\mu_k - 8\mu_k - 4\sqrt{2}\mu_k^2 > 0. \quad (47)$$

The left hand side above is an increasing function of b , and due to the condition (46) we plug in $b = 4\mu$. Hence, (47) reduces to

$$\mu_k^2 > 0.$$

obviously satisfied for all μ . \square

Our eventual estimate for T^{-1} relies on computing all of its components explicitly, and then bounding the resulting sum. The explicit formulas for T^{-1} are build using the recursive formulas presented in Def. 3.5. For further details refer to [20].

Lemma 3.9. *Let $n < \frac{N}{2}$. The $N - 2n \times N - 2n$ top left corner submatrix of T^{-1} is given explicitly by*

$$T^{-1}(d_1, d_2, \dots, d_{N-2n} + \mu_k^2 a_n),$$

whereas the $2n \times 2n$ bottom right corner submatrix of T^{-1} is given explicitly by

$$T^{-1}(d_{N-2n+1} + \mu_k^2 b_{\frac{N-2n}{2}}, d_{N-2n+2}, \dots, d_N),$$

where a_j and $b_{\frac{N-2j-2}{2}}$ are elements of the recursive series from Def. 3.5.

Proof. Follows from Lemma 3.4 with $R = T(d_1, d_2, \dots, d_{N-2n})$, and $F = T(d_{N-2n+1}, d_{N-2n+2}, \dots, d_N)$, and computing the recursion for the elements R_{11}^{-1} and F_{nn}^{-1} . For the detailed proof refer to [20]. \square

We have the following corollary from Lemma 3.9

Corollary 3.10. *The 2×2 dimensional diagonal blocks of T^{-1} are given by*

$$\begin{bmatrix} d_{N-2j-1} + \mu_k^2 b_{\frac{N-2j-2}{2}} & \mu_k \\ -\mu_k & d_{N-2j} + \mu_k^2 a_j \end{bmatrix}^{-1}$$

for $j = 0, \dots, \frac{N}{2} - 1$, where a_j and $b_{\frac{N-2j-2}{2}}$ are elements of the recursive series from Def. 3.5. Observe that $j = 0$ denotes the bottom-right T^{-1} diagonal block.

Theorem 3.11. *Consider the $2n \times 2n$ dimensional bottom right corner square submatrix of T^{-1}*

$$\tilde{T}^{-1} \stackrel{\text{def}}{=} T(d_{N-2n+1} + \mu_k^2 b_{\frac{N-2n}{2}}, d_{N-2n+2}, \dots, d_N)^{-1}.$$

The following recursive explicit formulas hold

$$\begin{aligned} \tilde{T}_{row(1:2), col(1:2)}^{-1} &= \tilde{I}, \\ \tilde{T}_{row(3:4), col(1:2)}^{-1} &= \mu_k \begin{bmatrix} -a_{n-1} \\ \hat{a}_{n-1} \end{bmatrix} \tilde{T}_{row(2), col(1:2)}^{-1}, \\ &\dots \\ \tilde{T}_{row(2j+1:2j+2), col(1:2)}^{-1} &= \mu_k \begin{bmatrix} -a_{n-j} \\ \hat{a}_{n-j} \end{bmatrix} \tilde{T}_{row(2j), col(1:2)}^{-1} \end{aligned}$$

where

$$\begin{aligned} \tilde{I} &\stackrel{\text{def}}{=} \begin{bmatrix} d_{N-2n+1} + \mu_k^2 b_{\frac{N-2n}{2}} & \mu_k \\ -\mu_k & d_{N-2n+2} + \mu_k^2 a_{n-1} \end{bmatrix}^{-1} = \\ &\frac{1}{(d_{N-2n+2} + \mu_k^2 a_{n-1})(d_{N-2n+1} + \mu_k^2 b_{\frac{N-2n}{2}}) + \mu_k^2} \begin{bmatrix} d_{N-2n+2} + \mu_k^2 a_{n-1} & \mu_k \\ -\mu_k & d_{N-2n+1} + \mu_k^2 b_{\frac{N-2n}{2}}, \end{bmatrix} \end{aligned} \quad (48)$$

is the inverse diagonal block, see Cor. 3.10, and $\{a_i\}_{i=1}^{N/2}$, $\{\hat{a}_i\}_{i=1}^{N/2}$ and $\{b_i\}_{i=1}^{N/2}$ are the recursive series from Def. 3.5.

Proof. We decompose into blocks

$$\tilde{T}^{-1} = \begin{bmatrix} T(d_{N-2n+1} + \mu_k^2 b_{\frac{N-2n}{2}}, d_{N-2n+2}, \dots, d_{N-2}) & -\mu_k \\ \mu_k^T & T(d_{N-1}, d_N) \end{bmatrix}^{-1} = \begin{bmatrix} \text{Inv}_{11}^{(1)} & \text{Inv}_{12}^{(1)} \\ \text{Inv}_{21}^{(1)} & \text{Inv}_{22}^{(1)} \end{bmatrix}.$$

We apply Lemma 3.4 with $F = T(d_{N-2n+1} + \mu_k^2 b_{\frac{N-2n}{2}}, d_{N-2n+2}, \dots, d_{N-2})$, and $R = T(d_{N-1}, d_N)$. It follows that

$$\begin{aligned} \text{Inv}_{11}^{(1)} &= \left(T(d_{N-2n+1} + \mu_k^2 b_{\frac{N-2n}{2}}, d_{N-2n+2}, \dots, d_{N-2}) + \mu_k \mu_k^T T_{11}^{-1}(d_{N-1}, d_N) \right)^{-1} = \\ &= T^{-1}(d_{N-2n+1} + \mu_k^2 b_{\frac{N-2n}{2}}, d_{N-2n+2}, \dots, d_{N-2} + \mu_k^2 a_1). \end{aligned}$$

(observe that μ_k is $(N-2) \times 2$ dimensional matrix – set $n = N-2$ in (44)). It holds that

$$\text{Inv}_{21}^{(1)} = -T^{-1}(d_{N-1}, d_N) \mu_k^T \text{Inv}_{11}^{(1)}, \quad (\text{Inv}_{21}^{(1)})_{\text{col}(1:2)} = \mu_k \begin{bmatrix} -a_1 \\ \hat{a}_1 \end{bmatrix} (\text{Inv}_{11}^{(1)})_{\text{row}(N-2), \text{col}(1:2)}.$$

In order to compute $(\text{Inv}_{11}^{(1)})_{\text{row}(N-2), \text{col}(1:2)}$ we decompose $\text{Inv}_{11}^{(1)}$ into blocks further

$$\text{Inv}_{11}^{(1)} = \begin{bmatrix} \text{Inv}_{11}^{(2)} & \text{Inv}_{12}^{(2)} \\ \text{Inv}_{21}^{(2)} & \text{Inv}_{22}^{(2)} \end{bmatrix} = \begin{bmatrix} T(d_{N-2n+1} + \mu_k^2 b_{\frac{N-2n}{2}}, d_{N-2n+2}, \dots, d_{N-4}) & -\mu_k \\ \mu_k^T & T(d_{N-3}, d_{N-2}) + \mu_k^2 a_1 \end{bmatrix}^{-1}.$$

It holds that

$$\text{Inv}_{21}^{(2)} = -T^{-1}(d_{N-3}, d_{N-2} + \mu_k^2 a_1) \mu_k^T \text{Inv}_{11}^{(2)}.$$

Hence

$$(\text{Inv}_{11}^{(1)})_{\text{row}(N-3:N-2), \text{col}(1:2)} = (\text{Inv}_{21}^{(2)})_{\text{row}(1:2), \text{col}(1:2)} = \mu_k \begin{bmatrix} -a_2 \\ \hat{a}_2 \end{bmatrix} (\text{Inv}_{11}^{(2)})_{\text{row}(N-4), \text{col}(1:2)}.$$

Repeating this procedure we find

$$(\text{Inv}_{11}^{(2)})_{\text{row}(N-5:N-4), \text{col}(1:2)} = (\text{Inv}_{21}^{(3)})_{\text{row}(1:2), \text{col}(1:2)} = \mu_k \begin{bmatrix} -a_3 \\ \hat{a}_3 \end{bmatrix} (\text{Inv}_{11}^{(3)})_{\text{row}(N-6), \text{col}(1:2)},$$

and

$$(\text{Inv}_{11}^{(j)})_{\text{row}(N-2j-1:N-2j), \text{col}(1:2)} = (\text{Inv}_{21}^{(j-1)})_{\text{row}(1:2), \text{col}(1:2)} = \mu_k \begin{bmatrix} -a_{j+1} \\ \hat{a}_{j+1} \end{bmatrix} (\text{Inv}_{11}^{(j-1)})_{\text{row}(N-2j-2), \text{col}(1:2)},$$

and finally (after several steps of recursion)

$$\begin{aligned} \text{Inv}_{21}^{(n-1)} &= -\tilde{I} \cdot \mu_k^T \text{Inv}_{11}^{(n-1)}, \quad \text{Inv}_{21}^{(n-1)} = \mu_k \begin{bmatrix} -a_{n-1} \\ \hat{a}_{n-1} \end{bmatrix} (\text{Inv}_{11}^{(n-1)})_{\text{row}(2)} \\ \text{Inv}_{11}^{(n-1)} &= \tilde{I} = T^{-1}(d_{N-2n+1} + \mu_k^2 b_{\frac{N-2n}{2}}, d_{N-2n+2} + \mu_k^2 a_{n-1}). \end{aligned} \quad (49)$$

We emphasize that the recursion is being finished here as $\text{Inv}_{11}^{(n-1)}$ is the 2×2 upper left corner matrix of T^{-1} . Observe that $T_{\text{row}(N-2j-1:N-2j), \text{col}(1:2)}^{-1} = (\text{Inv}_{11}^{(j)})_{\text{row}(N-2j-1:N-2j), \text{col}(1:2)}$ for $j = 1, \dots, n-1$. Therefore we obtained the claim. \square

Remark 3.12. By repetitive application of Thm. 3.11 we obtain the explicit formulas for all values of the lower triangle of the full tridiagonal inverse matrix T^{-1} (43). E.g. by setting $n = \frac{N}{2}$ in Thm. 3.11 we obtain the formulas for the first and the second columns of T^{-1} , and so on.

Lemma 3.13. *Matrix T^{-1} satisfies the following symmetries*

$$\begin{aligned} T_{j+2i,j}^{-1} &= T_{j,j+2i}^{-1}, \quad T_{j+2i+1,j}^{-1} = -T_{j,j+2i+1}^{-1}, \\ T_{j-2i,j}^{-1} &= T_{j,j-2i}^{-1}, \quad T_{j-2i+1,j}^{-1} = -T_{j,j-2i+1}^{-1}. \end{aligned}$$

for all $1 \leq j \leq N$ and $i > 0$ such that $j + 2i + 1 \leq N$, and $1 \leq j - 2i + 1$.

Proof. Without loss of generality, let $1 \leq j \leq N$. It must hold that

$$T_{j-1,j}^{-1} T_{j,j-1} + T_{j,j}^{-1} T_{j,j} + T_{j+1,j}^{-1} T_{j,j+1} = 1, \quad T_{j,j-1}^{-1} T_{j-1,j} + T_{j,j}^{-1} T_{j,j} + T_{j,j+1}^{-1} T_{j+1,j} = 1,$$

as it holds that $T_{j,j-1} = -T_{j-1,j}$ and $T_{j,j+1} = -T_{j+1,j}$ we obtain

$$T_{j-1,j}^{-1} = -T_{j,j-1}^{-1} \quad \text{and} \quad T_{j+1,j}^{-1} = -T_{j,j+1}^{-1}. \quad (50)$$

From the same argument applied to other column we get

$$T_{j,j}^{-1} T_{j+1,j} + T_{j+1,j}^{-1} T_{j+1,j+1} + T_{j+2,j}^{-1} T_{j+1,j+2} = 0, \quad T_{j,j}^{-1} T_{j,j+1} + T_{j,j+1}^{-1} T_{j+1,j+1} + T_{j,j+2}^{-1} T_{j+2,j+1} = 0.$$

From (50) and $T_{j+1,j+2} = -T_{j+2,j+1}$ it follows that $T_{j+2,j}^{-1} = T_{j,j+2}^{-1}$.

Now, it is clearly seen that proceeding further analogously we obtain the claim. \square

Remark 3.14. *By iterative application of Thm. 3.11 we can obtain the explicit formulas for all values of the lower triangle of the full tridiagonal inverse matrix T^{-1} (43). Then, the symmetries from Lemma 3.13 provides the explicit formulas for all values of the full tridiagonal inverse matrix T^{-1} .*

To show the main result about the bound for the inverse tridiagonal operator, i.e. Theorem 3.3 we will use the following auxiliary lemmas providing bounds for the recursive series defined previously. We have the following estimate for the submatrix of T^{-1} that we consider a 'tail'.

Lemma 3.15. *Let $N > 2\mu_k$. For any $1 \leq i \leq 2\mu_k$, it holds that*

$$\left\| T_{\text{row}(2\lfloor\mu_k\rfloor+1:N), \text{col}(i)}^{-1} \right\|_{\ell^1} \leq \frac{1}{\mu_k}.$$

Proof. Let $i = N - 2n + 1$. Consider \tilde{T}^{-1} the $2n \times 2n$ bottom right corner submatrix of T_k^{-1}

$$\tilde{T}^{-1} = T(d_{N-2n+1} + \mu_k^2 b_{\frac{N-2n}{2}}, d_{N-2n+2}, \dots, d_N)^{-1}.$$

Recall the recurrence relation shown in Thm. 3.11

$$\tilde{T}_{\text{row}(2j+1:2j+2), \text{col}(1:2)}^{-1} = \mu_k \begin{bmatrix} -a_{n-j} \\ \hat{a}_{n-j} \end{bmatrix} \tilde{T}_{\text{row}(2j), \text{col}(1:2)}^{-1}. \quad (51)$$

As \tilde{T}^{-1} is the bottom right corner submatrix of T^{-1} , we can easily map (51) to the full matrix T^{-1} , and we have

$$T_{\text{row}(l+2j+1:l+2j+2), \text{col}(l+1:l+2)}^{-1} = \mu_k \begin{bmatrix} -a_{n-j} \\ \hat{a}_{n-j} \end{bmatrix} T_{\text{row}(l+2j), \text{col}(l+1:l+2)}^{-1},$$

where $l = N - 2n$. After unveiling the recurrence relation we obtain for $c \in \{1, 2\}$

$$\left| T_{\text{row}(l+2j+1:l+2j+2), \text{col}(l+c)}^{-1} \right| = \begin{cases} \mu_k^j (a_{n-j} + \hat{a}_{n-j}) \prod_{l=1}^{j-1} \hat{a}_{n-l} |\tilde{I}_{2c}| & \text{for } j > 1, \\ \mu_k (a_{n-1} + \hat{a}_{n-1}) |\tilde{I}_{2c}| & \text{for } j = 1, \\ |\tilde{I}_{\text{row}(c)}| & \text{for } j = 0. \end{cases} \quad (52)$$

where \tilde{I} is given by (48). Therefore after summing up we have

$$\begin{aligned} \left| T_{row(l+2j+1:N), col(l+c)}^{-1} \right|_{\ell^1} &= \mu_k^j (a_{n-j} + \hat{a}_{n-j}) \prod_{l=1}^{j-1} \hat{a}_{n-l} |\tilde{I}_{2c}| + \mu_k^{j+1} (a_{n-j-1} + \hat{a}_{n-j-1}) \prod_{l=1}^j \hat{a}_{n-l} |\tilde{I}_{2c}| \\ &\quad + \cdots + \mu_k^{n-1} (a_1 + \hat{a}_1) \prod_{l=1}^{n-2} \hat{a}_{n-l} |\tilde{I}_{2c}|. \end{aligned} \quad (53)$$

for $j > 1$ (in cases of $j = 1$ we add the additional term $\mu_k (a_{n-1} + \hat{a}_{n-1}) |\tilde{I}_{2c}|$ appearing in (52)). We obtain exactly the formula from the statement of the theorem by setting $l + 2j + 1 = 2\lfloor \mu_k \rfloor + 1$ above. Also, $|\tilde{I}_{21}|, |\tilde{I}_{22}|$ satisfy the bounds (see Lem. 3.7)

$$|\tilde{I}_{21}| = \frac{\mu_k}{(d_{N-2n+1} + \mu_k^2 b_{\frac{N-2n}{2}})(d_{N-2n+2} + \mu_k^2 a_{n-1}) + \mu_k^2} \leq \hat{a}_n < \frac{1}{\mu_k}, \quad (54a)$$

$$|\tilde{I}_{22}| = \frac{d_{N-2n+1} + \mu_k^2 b_{\frac{N-2n}{2}}}{(d_{N-2n+1} + \mu_k^2 b_{\frac{N-2n}{2}})(d_{N-2n+2} + \mu_k^2 a_{n-1}) + \mu_k^2} \leq b_{\frac{N-2n+2}{2}} < \frac{1}{\mu_k}. \quad (54b)$$

for all j such that

$$l + 2j + 1 \geq \lfloor \mu_k \rfloor, \quad (55)$$

observe that the assumption of Lem. 3.8, i.e. $n - j \leq \frac{N}{2} - \lfloor \mu_k \rfloor$, follows from (55), and hence it holds that

$$\hat{a}_{n-j} + a_{n-j} \leq \frac{1}{2\mu_k}, \text{ and for } j > 1 \quad \prod_{l=1}^{j-1} \hat{a}_{n-l} \leq \frac{1}{4^{j-1} \mu_k^{j-1}},$$

and hence all terms from (53) are bounded by

$$\begin{aligned} \mu_k^j (a_{n-j} + \hat{a}_{n-j}) \prod_{l=1}^{j-1} \hat{a}_{n-l} |\tilde{I}_{21}| &< \mu_k^j \frac{1}{2\mu_k} \frac{1}{4^{j-1} \mu_k^{j-1}} \frac{1}{\mu_k} = \frac{1}{2^{2j-1} \mu_k}, \text{ for } j > 1, \\ \mu_k (a_{n-1} + \hat{a}_{n-1}) |\tilde{I}_{2c}| &< \frac{1}{2\mu_k}. \end{aligned}$$

and summing the terms above we obtain the claim. \square

At this point the provided auxiliary lemmas allow us to derive a computer-assisted proof of the main result in the form of the following theorems. A Theorem is provided for each studied PDE separately, the PDEs are presented in detail in Section 5.

Remark 3.16. We precompute explicit bounds for $\|T_k^{-1}\|_{B(\ell^1)}$ as a function of μ_k (using a grid of intervals of length 1) and for $N = 2\mu_k$. The bounds are computed using a C++ program included in the supplementary material, and saved as a .csv file included in the supplementary materials. Then multiplying the resulting values by $k^{d/3}$ corresponding to μ_k defined by the PDE, we obtain an upper bound for $\|k^{d/3} \cdot T_k^{-1}\|_{B(\ell^1)}$. This step is equation and time-step dependent (μ depends on the eigenvalues in the PDE and the time-step h). According to Lemma 3.15, the tail outside the block of size $2\mu_k$ is bounded uniformly. Therefore, we obtain the bound for $\|k^{d/3} \cdot T_k^{-1}\|_{B(\ell^1)}$ uniform with respect to μ_k by combining the finite block and tail bounds.

Theorem 3.17 (KS equation). *Let T_k be the tridiagonal operator (3.3), where the off-diagonal terms μ_k are defined by the linear operator of the Kuramoto-Sivashinsky PDE, i.e. $\mu_k = \frac{h}{2} \cdot \alpha (k^4 - k^2)$. For all k*

such that $\mu_k \geq 30000$, the following upper bounds for $\|\tilde{k}^{d/3} \cdot T_k^{-1}\|_{B(\ell^1)}$ hold

1. Let $\alpha \cdot h \geq \frac{1}{375}$, then $\|\tilde{k}^{d/3} \cdot T_k^{-1}\|_{B(\ell^1)} \leq 3.74$
2. Let $\alpha \cdot h \geq \frac{2}{1125}$, then $\|\tilde{k}^{d/3} \cdot T_k^{-1}\|_{B(\ell^1)} \leq 5.63$
3. Let $\alpha \cdot h \geq \frac{1}{2250}$, then $\|\tilde{k}^{d/3} \cdot T_k^{-1}\|_{B(\ell^1)} \leq 49.26$

Theorem 3.18 (Fisher equation). Let T_k be the tri-diagonal operator (3.3), where the off-diagonal terms μ_k are defined by the linear operator of the Fisher PDE, i.e. $\mu_k = \frac{h}{2} (k^2 - \alpha)$.

Let $h \geq 0.002$ and $\alpha \leq 30000$, then it holds that $\|\tilde{k}^{d/3} \cdot T_k^{-1}\|_{B(\ell^1)} \leq 5.11$.

Theorem 3.19 (Swift-Hohenberg equation). Let T_k be the tridiagonal operator (3.3), where the off-diagonal terms μ_k are defined by the linear operator of the Swift-Hohenberg PDE, i.e. $\mu_k = \frac{h}{2} (k^4 - 2k^2 - \alpha + 1)$.

Let $h \geq 0.002$ and $\alpha \leq 20000$, then it holds that $\|\tilde{k}^{d/3} \cdot T_k^{-1}\|_{B(\ell^1)} \leq 5.11$.

Theorem 3.20 (PFC equation). Let T_k be the tri-diagonal operator (3.3), where the off-diagonal terms μ_k are defined by the linear operator of the PFC PDE, i.e. $\mu_k = \frac{h}{2} [k^6 - 2k^4 - (\alpha + 1)k^2]$, the following upper bounds for $\|\tilde{k}^{d/3} \cdot T_k^{-1}\|_{B(\ell^1)}$ hold

1. Let $h \geq 0.002$ and $\alpha \leq 100$, then it holds that $\|\tilde{k}^{d/3} \cdot T_k^{-1}\|_{B(\ell^1)} \leq 5.5$
2. Let $h \geq 0.0005$ and $\alpha \leq 250$, then it holds that $\|\tilde{k}^{d/3} \cdot T_k^{-1}\|_{B(\ell^1)} \leq 36.82$

Remark 3.21. The rationale of splitting the main result Thm. 3.17 and 3.20 into several cases depending on the lower bound for $\alpha \cdot h$ is that the proof becomes harder numerically when the time step h decreases (keeping α constant). This is consistent with the fact that $\tilde{k}^{d/3} \cdot T_k^{-1}$ matrix becomes unbounded as $h \rightarrow 0$.

Proof of Thm. 3.17 (and analogous for other PDEs). The proof is computer-assisted. We present the details in Appendix A. Let us describe a sketch of the proof having a numerical part implemented in the C++ language and a symbolic part implemented in the Mathematica language [26]. We directly employ the recursive formulas derived for all entries of T_k^{-1} from Thm. 3.11 and the symmetry from Lem. 3.13. Using the formulas we derive an explicit upper bound for $\|\tilde{k}^{d/3} \cdot T_k^{-1}\|_{B(\ell^1)}$ as a function of its dimension equal to $2\mu_k$. An upper bound for $\|\tilde{k}^{d/3} \cdot T_k^{-1}\|_{B(\ell^1)}$ is obtained by adding the tail estimate derived in Lem. 3.15 to obtain an upper bound for sufficiently large μ_k 's.

The computer-assisted proof consists of several steps. First, using a C++ code employing interval arithmetic computation, we bound $\|\tilde{k}^{d/3} \cdot T_k^{-1}\|_{B(\ell^1)}$ for a finite number of μ_k values up to some large $\bar{\mu}_k$. Finally, in large μ_k regime ($\mu_k > \bar{\mu}_k$) we use symbolic computation coded in Mathematica. We compute a symbolic representation of M – an explicit global upper bound for all entries of $\tilde{k}^{d/3} \cdot T_k^{-1}$. Using the explicit bound M , we bound $\|\tilde{k}^{d/3} \cdot T_k^{-1}\|_{B(\ell^1)}$ by $M^{C\mu_k^{1/2}}$. Eventually we show that the limit $M^{C\mu_k^{1/2}}$ as $\mu_k \rightarrow \infty$ exists and is decreasing with μ_k , hence the final upper bound for $\mu_k > \bar{\mu}_k$ is given by a computable number $M^{C\mu_k^{1/2}}$.

□

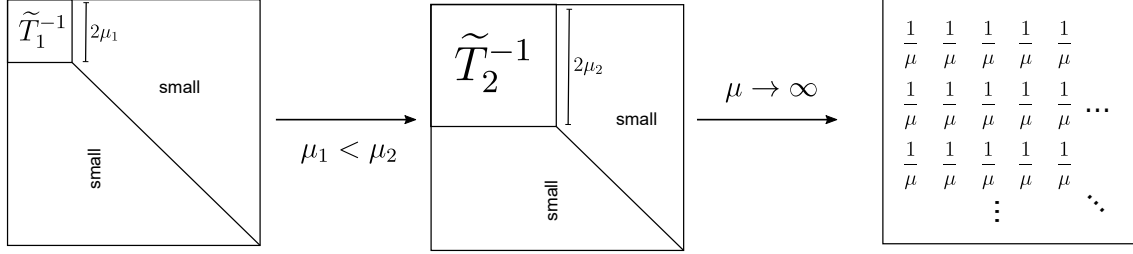


Figure 3: Diagram motivating requirement of performing our analysis to compute the stability of the inverse tridiagonal operator T_k^{-1} with respect to the approximation dimension. Notation \tilde{T}_1, \tilde{T}_2 mean the upper left finite dimensional block of T_k^{-1} having μ_1, μ_2 as the off-diagonal elements, which are denoted by $(T_k^{-1})_{row(1,2\mu), col(1,2\mu)}$. Intuitively, all the entries of the inverse matrices outside \tilde{T}_1 and \tilde{T}_2 are small, as they lie in the regime where the corresponding part of T_k is diagonally dominant.

3.2.2 Inverse full linear operator norm $\|\mathcal{L}_k^{-1}\|_{B(\ell^1)}$

We are going to use the following well known result in linear algebra about the inverse of the sum of an invertible matrix A and a rank one perturbation uv^T (u, v are vectors), known as the *Sherman-Morrison formula* [27, 28, 29, 30, 31].

Lemma 3.22 ([31]). *Suppose A is an invertible real square matrix and u, v are column vectors. Suppose furthermore that $1 + v^T A^{-1} u \neq 0$. Then the Sherman-Morrison formula states that*

$$(A + uv^T)^{-1} = A^{-1} - \frac{A^{-1}uv^TA^{-1}}{1 + v^TA^{-1}u}.$$

Here, uv^T is the outer product of two vectors u and v .

The more general general version of this result for rank k perturbations UV (U is $n \times k$ dim. matrix, V is $k \times n$ dim. matrix)

Lemma 3.23 ([29, 30]). *Suppose A is an invertible real square matrix and U is $n \times k$ matrix, V is $k \times n$ matrix. Suppose furthermore that $I + VA^{-1}U$ is invertible. Then the Woodbury formula states that*

$$(A + UV)^{-1} = A^{-1} - A^{-1}U(I + VA^{-1}U)^{-1}VA^{-1}$$

Now let us apply Lemma 3.22 for the inverse of the linear operator that we consider. We recall its form below. \mathcal{L}_k is being decomposed into a sum of a tridiagonal matrix and a rank one matrix, i.e.

$$\mathcal{L}_k = M_k + U = \begin{bmatrix} 1 & 0 & \cdots & 0 \\ \mu_k \tilde{k}^{-d/3} & \tilde{k}^{-d/3} \cdot T_k & & \\ 0 & & & \\ \vdots & & & \end{bmatrix} + \begin{bmatrix} 0 & -2 & 2 & \cdots \\ & 0 & & \\ & & & \end{bmatrix}, \quad (56)$$

where

$$T_k = \begin{bmatrix} 2 & -\mu_k & 0 & \cdots & \\ \mu_k & 4 & -\mu_k & 0 & \cdots \\ \ddots & \ddots & \ddots & \ddots & \ddots \\ \cdots & 0 & \mu_k & 2(N-1) & -\mu_k \\ & \cdots & 0 & \mu_k & 2N \end{bmatrix} \quad (57)$$

Observe that in our case, we apply the Sherman-Morrison formula for (56), and we put

$$A + uv^T = \mathcal{L}_k^{-1}, \quad A = M_k, \quad uv^T = U, \quad u = [1, 0, \dots, 0]^T, \quad v^T = 2 [0, -1, 1, \dots, (-1)^{k+1}, \dots].$$

M_k is invertible, being a tridiagonal matrix it can be checked by the recursive determinant computation, that it is bounded away from zero for all k and N .

Lemma 3.24. *The inverse of M_k in (41) is given by*

$$M_k^{-1} = \begin{bmatrix} 1 & 0 \\ \mu_k \tilde{k}^{-d/3} & \tilde{k}^{-d/3} \cdot T_k \\ 0 & \vdots \\ \vdots & \tilde{k}^{-d/3} \cdot T_k \end{bmatrix}^{-1} = \begin{bmatrix} 1 & 0 & \cdots & 0 \\ -\mu_k (T_k^{-1})_{col(1)} & \tilde{k}^{d/3} \cdot T_k^{-1} & & \end{bmatrix}. \quad (58)$$

Proof. Let us denote $\text{Inv} \stackrel{\text{def}}{=} M_k^{-1}$. From solving the linear system of equations

$$\begin{bmatrix} 1 & 0 \\ \mu_k \tilde{k}^{-d/3} & \tilde{k}^{-d/3} \cdot T_k \\ 0 & \vdots \\ \vdots & \tilde{k}^{-d/3} \cdot T_k \end{bmatrix} \cdot \begin{bmatrix} \text{Inv}_{11} & \text{Inv}_{12} \\ \text{Inv}_{21} & \text{Inv}_{22} \end{bmatrix} = \begin{bmatrix} 1 & 0 \\ 0 & \text{Id} \end{bmatrix}.$$

we have that

$$\begin{aligned} \text{Inv}_{11} &= 1, & \text{Inv}_{12} &= 0, \\ \text{Inv}_{21} &= T_k^{-1} \begin{bmatrix} -\mu_k \\ 0 \\ \vdots \\ 0 \end{bmatrix} = -\mu_k (T_k^{-1})_{col(1)}, & \text{Inv}_{22} &= \tilde{k}^{d/3} \cdot T_k^{-1}. \end{aligned}$$

□

Corollary 3.25. *Let M_k be the first term in the decomposition of \mathcal{L}_k in (56).*

$$\mathcal{L}_k^{-1} = M_k^{-1} - \frac{M_k^{-1} U M_k^{-1}}{1 + v^T M_k^{-1} u}. \quad (59)$$

Theorem 3.26. *Let $\mu_k > 0$. Let T_k be the tridiagonal operator (3.3), and \mathcal{L}_k be the finite dimensional operator having the diagonal block structure as in (56).*

For all k such that $\mu_k \geq 0$ and for all N it holds that

$$\|\mathcal{L}_k^{-1}\|_{B(\ell^1)} \leq \max \left\{ 3 \left\| \tilde{k}^{d/3} \cdot T_k^{-1} \right\|_{B(\ell^1)}, 1 \right\}.$$

Proof. We denote

$$[a_{ij}]_{i,j=1}^{N+1} = M_k^{-1} = \begin{bmatrix} 1 & 0 & \cdots & 0 \\ -\mu_k (T_k^{-1})_{col(1)} & \tilde{k}^{d/3} \cdot T_k^{-1} & & \end{bmatrix}. \quad (60)$$

First, we recall the explicit form of \mathcal{L}^{-1} (59)

$$\mathcal{L}_k^{-1} = M_k^{-1} - \frac{M_k^{-1} U M_k^{-1}}{1 + v^T M_k^{-1} u}. \quad (61)$$

Observe that

$$M_k^{-1} U M_k^{-1} = M_k^{-1} u v^T M_k^{-1} = 2 \begin{bmatrix} a_{11} \\ a_{21} \\ \vdots \\ a_{n1} \end{bmatrix} \cdot \begin{bmatrix} \sum_{j=2}^{n+1} (-1)^{j+1} a_{j,1} & \sum_{j=2}^{n+1} (-1)^{j+1} a_{j,2} & \cdots & \sum_{j=2}^{n+1} (-1)^{j+1} a_{j,n+1} \end{bmatrix}$$

and

$$1 + v^T M_k^{-1} u = 1 + 2 \sum_{j=2}^{\infty} (-1)^{j+1} a_{j,1}.$$

We will bound $\|(\mathcal{L}_k^{-1})_{col(l)}\|_{B(\ell^1)}$ by considering two cases. First, we consider the case of $(\mathcal{L}_k^{-1})_{col(l)}$ for $l \geq 2$

$$(\mathcal{L}_k^{-1})_{col(l)} = \left(a_{i,l} - 2 \frac{a_{i,1} \sum (-1)^{j+1} a_{j,l}}{1 + 2 \sum (-1)^{j+1} a_{j,1}} \right)_{i=1}^{\infty} = \left(\frac{a_{i,l} + 2a_{i,l} \sum (-1)^{j+1} a_{j,1} - 2a_{i,1} \sum (-1)^{j+1} a_{j,l}}{1 + 2 \sum (-1)^{j+1} a_{j,1}} \right)_{i=1}^{\infty}. \quad (62)$$

Now taking the absolute value of each entry of the vector (62), applying the triangle inequality, and summing up we obtain the following estimate for the $B(\ell^1)$ norm

$$\|(\mathcal{L}_k^{-1})_{col(l)}\|_{\ell^1} \leq \frac{\sum_i |a_{i,l}| + 2 \sum_i |a_{i,l}| \sum_j |a_{j,1}| + 2 \sum_j |a_{j,l}| (1 + \sum_j |a_{j,1}|)}{|1 + 2 \sum (-1)^{j+1} a_{j,1}|} = \frac{\sum_i |a_{i,l}| (1 + 4 \sum_j |a_{j,1}| + 2)}{|1 + 2 \sum (-1)^{j+1} a_{j,1}|},$$

where we used the notation $\sum_i = \sum_{i=1}^{n+1}$ and $\sum_j = \sum_{j=2}^{n+1}$. Because, the first element of the first column of A_k^{-1} is equal to 1 (see (60)) it holds that $1 + \sum_j |a_{j,1}| = \sum_i |a_{i,1}|$, and $\sum_j |a_{j,l}| = \sum_i |a_{i,l}|$ for $l \geq 2$. Knowing the explicit formulas of elements in $(T_k^{-1})_{col(1)}$ with precise sign information from Lem. 3.13, we obtain that

$$\sum_{j=2}^{\infty} (-1)^{j+1} a_{j,1} = \sum_{j=1}^{\infty} |\mu_k (T_k^{-1})_{j,1}| = |\mu_k| \| (T_k^{-1})_{col(1)} \|_{B(\ell^1)}. \quad (63)$$

Now, using the explicit form of A^{-1} (61), we obtain

$$\|(\mathcal{L}_k^{-1})_{col(l)}\|_{B(\ell^1)} \leq \frac{\|\tilde{k}^{d/3} \cdot T_k^{-1}\|_{B(\ell^1)} (3 + 4|\mu_k| \| (T_k^{-1})_{col(1)} \|_{B(\ell^1)})}{1 + 2|\mu_k| \| (T_k^{-1})_{col(1)} \|_{B(\ell^1)}}.$$

for all $l \geq 2$, and therefore

$$\|(\mathcal{L}_k^{-1})_{col(2,N+1)}\|_{B(\ell^1)} \leq 2 \|\tilde{k}^{d/3} \cdot T_k^{-1}\|_{B(\ell^1)} + \frac{\|\tilde{k}^{d/3} \cdot T_k^{-1}\|_{B(\ell^1)}}{1 + 2|\mu_k| \| (T_k^{-1})_{col(1)} \|_{B(\ell^1)}} \leq 3 \|\tilde{k}^{d/3} \cdot T_k^{-1}\|_{B(\ell^1)}.$$

For the case of $j = 1$ we proceed differently

$$(\mathcal{L}_k^{-1})_{B(\ell^1)} = \left(a_{i,1} - 2 \frac{a_{i,1} \sum (-1)^{j+1} a_{j,1}}{1 + 2 \sum (-1)^{j+1} a_{j,1}} \right)_{i=1}^{\infty} = \left(\frac{a_{i,1}}{1 + 2 \sum (-1)^{j+1} a_{j,1}} \right)_{i=1}^{\infty}. \quad (64)$$

Using again the explicit form of $(T_k^{-1})_{col(1)}$ we get (using also (63))

$$\|(\mathcal{L}_k^{-1})_{col(1)}\|_{B(\ell^1)} \leq \frac{1 + |\mu_k| \| (T_k^{-1})_{col(1)} \|_{B(\ell^1)}}{1 + 2|\mu_k| \| (T_k^{-1})_{col(1)} \|_{B(\ell^1)}} \leq 1$$

and finally we obtain the claim. \square

We have the following straightforward corollary summarizing results derived in this section.

Corollary 3.27. *The following explicit upper bound holds $\|\mathcal{L}_k^{-1}\|_{B(\ell^1)} \leq 3 \|\tilde{k}^{d/3} \cdot T_k^{-1}\|_{B(\ell^1)}$, where the bound for $\|\tilde{k}^{d/3} \cdot T_k^{-1}\|_{B(\ell^1)}$ (always greater than 1) is defined by the studied PDE and provided in Theorems 3.17, 3.18, 3.19, 3.20.*

3.3 Bound for $\|\mathcal{L}^{-1}\|_{B(X_{\nu,1})}$

Recall from Lemma 3.1 the definitions of ρ_k and β_k given in (36) and (37), respectively. Assume that we have computed the bounds $\|\mathcal{L}_k^{-1}\|_{B(\ell^1)} \leq \frac{\beta_k}{1-\rho_k}$ for $k = k_0, \dots, \hat{k}$ using the computer-assisted approach of Section 3.1. Denote by $\tilde{\delta}$ the uniform bounds for $\|\mathcal{L}_k^{-1}\|_{B(\ell^1)}$ for large k from Section 3.2. Depending on the PDE model under consideration, this uniform bound is obtained by combining the database of estimates as alluded to in Remark 3.16 and the theoretical result of Theorem 3.18, Theorem 3.17, Theorem 3.19 or Theorem 3.20. Letting

$$\delta \stackrel{\text{def}}{=} \max \left(\max_{k=k_0, \dots, \hat{k}} \frac{\beta_k}{1-\rho_k}, \tilde{\delta} \right), \quad (65)$$

we get the following result.

Lemma 3.28.

$$\|\mathcal{L}^{-1}\|_{X_{\nu,1}} \leq \delta. \quad (66)$$

Proof. Letting $a \in X_{\nu,1}$ such that $\|a\|_{X_{\nu,1}} \leq 1$, we get that

$$\begin{aligned} \|\mathcal{L}^{-1}a\|_{X_{\nu,1}} &= \delta_{k_0,0} \|\mathcal{L}_{k_0}^{-1}a_0\|_{\ell^1} + 2 \sum_{k \geq 1} \|\mathcal{L}_k^{-1}a_k\|_{\ell^1} \nu^k \\ &\leq \delta_{k_0,0} \|\mathcal{L}_{k_0}^{-1}\|_{B(\ell^1)} \|a_0\|_{\ell^1} + 2 \sum_{k \geq 1} \|\mathcal{L}_k^{-1}\|_{B(\ell^1)} \|a_k\|_{\ell^1} \nu^k \\ &\leq \max \left(\max_{k=k_0, \dots, \hat{k}} \|\mathcal{L}_k^{-1}\|_{B(\ell^1)}, \tilde{\delta} \right) \left(\delta_{k_0,0} \|a_0\|_{\ell^1} + 2 \sum_{k \geq 1} \|a_k\|_{\ell^1} \nu^k \right) \\ &\leq \delta \|h\|_{X_{\nu,1}} \leq \delta. \end{aligned}$$

□

4 Bounds for the radii polynomial

Recall that the hypothesis of Theorem 2.2 is verified using the radii polynomial $p(r)$ defined in (30). In this section, we present a constructive way to compute the bounds required to define $p(r)$, namely the bounds Y and $Z = Z(r)$ given by (28) and (29), respectively.

Assume that the initial condition is given as

$$b \in B_{r_0}(\bar{b}) = \{b \in \ell_{\nu}^1 : \|b - \bar{b}\|_{\ell_{\nu}^1} \leq r_0\},$$

given some $\nu \geq 1$ and r_0 the error bound. Typically the error bound r_0 will come from the radius of the radii polynomial from the previous rigorous integration step. In Section 4.3, we show how this bound can be obtained. Here, it is understood that for $b = (b_k)_{k \geq k_0}$,

$$\|b\|_{\ell_{\nu}^1} = \delta_{k_0,0} |b_0| + 2 \sum_{k \geq 1} |b_k| \nu^k.$$

In this section, we use the notation $F(a, b)$ instead of $F(a)$ to emphasize the dependency of the zero finding problem $F = 0$ (See (22)) in the initial condition $b \in \ell_{\nu}^1$.

Recall from Lemma 3.1 the definitions of ρ_k and β_k given in (36) and (37), respectively. Assume that we have computed the bounds $\|\mathcal{L}_k^{-1}\|_{B(\ell^1)} \leq \frac{\beta_k}{1-\rho_k}$ for $k = k_0, \dots, \hat{k}$ using the computer-assisted approach of Section 3.1. Denote by $\tilde{\delta}$ the uniform bounds for $\|\mathcal{L}_k^{-1}\|_{B(\ell^1)}$ for $k > \hat{k}$ from Section 3.2. In fact, depending on the model under consideration, we use the results from

We now present a strategy to compute each bound separately.

4.1 The bound Y

Recalling from (23) that $\mathcal{T}(a) \stackrel{\text{def}}{=} a - \mathcal{L}^{-1}F(a, b) = \mathcal{L}^{-1}(b - \frac{h}{2}\mathbf{K}^{-\tilde{n}}\mathbf{\Lambda}\mathcal{N}(a))$, note that Y satisfy

$$\|\mathcal{T}(\bar{a}) - \bar{a}\|_{X_{\nu,1}} = \|\mathcal{L}^{-1}F(\bar{a}, b)\|_{X_{\nu,1}} \leq Y.$$

Since the nonlinearity of the PDE is a polynomial and \bar{a} has only finitely many nonzero entries, there exists $M > \hat{k}$ such that $F_k(\bar{a}, \bar{b}) = 0$ for all $k > M$. Hence,

$$\begin{aligned} \|\mathcal{L}^{-1}F(\bar{a}, \bar{b})\|_{X_{\nu,1}} &= \delta_{k_0,0}\|\mathcal{L}_{k_0}^{-1}F_{k_0}(\bar{a}, \bar{b})\|_{\ell^1} + 2\sum_{k=1}^{\hat{k}}\|\mathcal{L}_k^{-1}F_k(\bar{a}, \bar{b})\|_{\ell^1}\nu^k + 2\sum_{k=\hat{k}+1}^M\|\mathcal{L}_k^{-1}F_k(\bar{a}, \bar{b})\|_{\ell^1}\nu^k \\ &\leq \delta_{k_0,0}\|\mathcal{L}_{k_0}^{-1}F_{k_0}(\bar{a}, \bar{b})\|_{\ell^1} + 2\sum_{k=1}^{\hat{k}}\|\mathcal{L}_k^{-1}F_k(\bar{a}, \bar{b})\|_{\ell^1}\nu^k + 2\tilde{\delta}\sum_{k=\hat{k}+1}^M\|F_k(\bar{a}, \bar{b})\|_{\ell^1}\nu^k. \end{aligned}$$

To compute a bound for $\|\mathcal{L}_k^{-1}F_k(\bar{a}, \bar{b})\|_{\ell^1}$ for $k = k_0, \dots, \hat{k}$, recall the definition of the approximate inverse A_k in Figure 1 and recall (40) in the proof of Lemma 3.1, that is

$$\mathcal{L}_k^{-1} = \left(\sum_{j \geq 0} (I - A_k \mathcal{L}_k)^j \right) A_k.$$

Hence, we get that

$$\|\mathcal{L}_k^{-1}F_k(\bar{a}, \bar{b})\|_{\ell^1} = \left\| \left(\sum_{j \geq 0} (I - A_k \mathcal{L}_k)^j \right) A_k F_k(\bar{a}, \bar{b}) \right\|_{\ell^1} \leq \frac{1}{1 - \rho_k} \|A_k F_k(\bar{a}, \bar{b})\|_{\ell^1}.$$

Hence, we can compute Y_0 such that

$$\begin{aligned} \|\mathcal{L}^{-1}F(\bar{a}, \bar{b})\|_{X_{\nu,1}} &\leq \delta_{k_0,0}\|\mathcal{L}_{k_0}^{-1}F_{k_0}(\bar{a}, \bar{b})\|_{\ell^1} + 2\sum_{k=1}^{\hat{k}}\|\mathcal{L}_k^{-1}F_k(\bar{a}, \bar{b})\|_{\ell^1}\nu^k + 2\tilde{\delta}\sum_{k=\hat{k}+1}^M\|F_k(\bar{a}, \bar{b})\|_{\ell^1}\nu^k \\ &\leq \delta_{k_0,0} \frac{\|A_0 F_0(\bar{a}, \bar{b})\|_{\ell^1}}{1 - \rho_0} + 2\sum_{k=1}^{\hat{k}} \frac{\|A_k F_k(\bar{a}, \bar{b})\|_{\ell^1}}{1 - \rho_k} \nu^k + 2\tilde{\delta}\sum_{k=\hat{k}+1}^M\|F_k(\bar{a}, \bar{b})\|_{\ell^1}\nu^k \\ &\leq Y_0. \end{aligned}$$

Moreover, recalling the definition of δ in (65), note that

$$\|\mathcal{L}^{-1}(b - \bar{b})\|_{X_{\nu,1}} \leq \|\mathcal{L}^{-1}\|_{B(X_{\nu,1})}\|b - \bar{b}\|_{X_{\nu,1}} = \|\mathcal{L}^{-1}\|_{B(X_{\nu,1})}\|b - \bar{b}\|_{\ell_\nu^1} \leq \delta r_0.$$

Finally, letting

$$Y \stackrel{\text{def}}{=} Y_0 + \delta r_0 \tag{67}$$

leads to the wanted bound as

$$\begin{aligned} \|\mathcal{T}(\bar{a}) - \bar{a}\|_{X_{\nu,1}} &= \|\mathcal{L}^{-1}F(\bar{a}, b)\|_{X_{\nu,1}} \\ &= \left\| \mathcal{L}^{-1} \left(\mathcal{L}\bar{a} - b + \frac{h}{2}\mathbf{K}^{-\tilde{n}}\mathbf{\Lambda}\mathcal{N}(\bar{a}) \right) \right\|_{X_{\nu,1}} \\ &\leq \left\| \mathcal{L}^{-1} \left(\mathcal{L}\bar{a} - \bar{b} + \frac{h}{2}\mathbf{K}^{-\tilde{n}}\mathbf{\Lambda}\mathcal{N}(\bar{a}) \right) \right\|_{X_{\nu,1}} + \|\mathcal{L}^{-1}(b - \bar{b})\|_{X_{\nu,1}} \\ &\leq \|\mathcal{L}^{-1}F(\bar{a}, \bar{b})\|_{X_{\nu,1}} + \delta r_0 \\ &\leq Y_0 + \delta r_0 = Y. \end{aligned}$$

Remark 4.1 (Wrapping effect). In the current set-up, the bound (67) inevitably leads to a quick wrapping effect, as the error from the previous step is multiplied by the factor δ , i.e. the upper bound (65) for $\|\mathcal{L}^{-1}\|_{B(X_{\nu,1})}$. To exemplify this, assume that δ is constant along the integration and that after the first step, $r_0 = \varepsilon$ (for some small $\varepsilon > 0$). In this case, we expect the error bound $r_0 \geq \delta^k \varepsilon$ at step $k > 1$. For instance, if $\varepsilon = 10^{-14}$ and if $\delta = 100$, then at step $k > 1$, the error bound should roughly be 10^{-14+2k} . Hence, expecting more than 7 successful steps in this case is probably too ambitious. See Tables 1, 2, 3 and 4 for some explicit data. That being said, we believe that a multi-steps approach should significantly fix this problem. This approach is currently part of future research.

4.2 The bound $Z(r)$

Recall from (29) that the bound $Z(r)$ satisfies

$$\sup_{c \in \overline{B_r(\bar{a})}} \|D_a \mathcal{T}(c)\|_{B(X_{\nu,1})} \leq Z(r).$$

The computation of the bound $Z(r)$ requires bounding the norm of some operators, which we do next.

Lemma 4.2. Recall the definition of the operator Λ in (20) and the block diagonal operator $\mathbf{\Lambda}$ in (21). Then $\mathbf{\Lambda} \in B(X_{\nu,1})$ with

$$\|\mathbf{\Lambda}\|_{B(X_{\nu,1})} \leq 2. \quad (68)$$

Proof. First, note that $\|\mathbf{\Lambda}\|_{B(X_{\nu,1})} \leq \|\Lambda\|_{B(\ell^1)}$, as for any $a \in X_{\nu,1}$ with $\|a\|_{X_{\nu,1}} \leq 1$,

$$\begin{aligned} \|\mathbf{\Lambda}a\|_{X_{\nu,1}} &= \delta_{k_0,0} \|\Lambda a_{k_0}\|_{\ell^1} + 2 \sum_{k \geq 1} \|\Lambda a_k\|_{\ell^1} \leq \delta_{k_0,0} \|\Lambda\|_{B(\ell^1)} \|a_{k_0}\|_{\ell^1} + 2 \sum_{k \geq 1} \|\Lambda\|_{B(\ell^1)} \|a_k\|_{\ell^1} \\ &\leq \|\Lambda\|_{B(\ell^1)} \left(\delta_{k_0,0} \|a_{k_0}\|_{\ell^1} + 2 \sum_{k \geq 1} \|a_k\|_{\ell^1} \right) \leq \|\Lambda\|_{B(\ell^1)} \|a\|_{X_{\nu,1}} \leq \|\Lambda\|_{B(\ell^1)}. \end{aligned}$$

Now, let $b \in \ell^1$ such that $\|b\|_{\ell^1} \leq 1$. Then, recalling the definition of the tridiagonal operator Λ in (20), the proof follows by observing that

$$\begin{aligned} \|\Lambda b\|_{\ell^1} &= 2 \sum_{k \geq 1} | -b_{k-1} + b_{k+1} | \leq 2|b_0| + 2 \sum_{k \geq 2} |b_{k-1}| + 2 \sum_{k \geq 1} |b_{k+1}| \\ &= \left(|b_0| + 2 \sum_{j \geq 1} |b_j| \right) + \left(|b_0| + 2 \sum_{j \geq 2} |b_j| \right) \leq 2\|b\|_{\ell^1} \leq 2. \quad \square \end{aligned}$$

Lemma 4.3. Assume that \hat{k} is a number such that $\lambda_k < 0$ for all $k \geq \hat{k}$.

$$\|\mathcal{L}^{-1} \mathbf{K}^{-\tilde{n}}\|_{B(X_{\nu,1})} \leq \sigma \stackrel{\text{def}}{=} \max \left(\max_{k=k_0, \dots, \hat{k}} \frac{1}{\tilde{k}^{\tilde{n}}} \frac{\beta_k}{1 - \rho_k}, \frac{\tilde{\delta}}{(\hat{k} + 1)^{\tilde{n}}} \right). \quad (69)$$

Proof. Let $a \in X_{\nu,1}$ such that $\|a\|_{X_{\nu,1}} \leq 1$. Then, recalling the definition of operator $\mathbf{K}^{-\tilde{n}}$ in (21),

$$\begin{aligned}
\|\mathcal{L}^{-1}\mathbf{K}^{-\tilde{n}}a\|_{X_{\nu,1}} &= \left\| \begin{pmatrix} \frac{1}{\tilde{k}_0^{\tilde{n}}} \mathcal{L}_{k_0}^{-1} a_{k_0} \\ \vdots \\ \frac{1}{\tilde{k}^{\tilde{n}}} \mathcal{L}_k^{-1} a_k \\ \vdots \end{pmatrix} \right\|_{X_{\nu,1}} \\
&= \frac{\delta_{k_0,0}}{\tilde{k}_0^{\tilde{n}}} \|\mathcal{L}_{k_0}^{-1} a_0\|_{\ell^1} + 2 \sum_{k \geq 1} \frac{1}{k^{\tilde{n}}} \|\mathcal{L}_k^{-1} a_k\|_{\ell^1} \nu^k \\
&\leq \frac{\delta_{k_0,0}}{\tilde{k}_0^{\tilde{n}}} \|\mathcal{L}_{k_0}^{-1}\|_{B(\ell^1)} \|a_0\|_{\ell^1} + 2 \sum_{k=1}^{\hat{k}} \frac{1}{k^{\tilde{n}}} \|\mathcal{L}_k^{-1}\|_{B(\ell^1)} \|a_k\|_{\ell^1} \nu^k + \frac{\tilde{\delta}}{(\hat{k}+1)^{\tilde{n}}} \left(2 \sum_{k>\hat{k}} \|a_k\|_{\ell^1} \nu^k \right) \\
&\leq \max \left(\max_{k=k_0, \dots, \hat{k}} \frac{1}{\tilde{k}^{\tilde{n}}} \|\mathcal{L}_k^{-1}\|_{B(\ell^1)}, \frac{1}{(\hat{k}+1)^{\tilde{n}}} \tilde{\delta} \right) \left(\delta_{k_0,0} \|a_0\|_{\ell^1} + 2 \sum_{k \geq 1} \|a_k\|_{\ell^1} \nu^k \right) \\
&\leq \sigma \|a\|_{X_{\nu,1}} \leq \sigma. \tag*{\square}
\end{aligned}$$

Lemma 4.4. *Let $\gamma(r)$ by any finite bound satisfying*

$$\sup_{c \in \overline{B_r(\bar{a})}} \|D_a \mathcal{N}(c)\|_{B(X_{\nu,1})} \leq \gamma(r). \tag{70}$$

Then

$$Z(r) \stackrel{\text{def}}{=} h\sigma\gamma(r) \tag{71}$$

satisfies (29).

Proof. The hypothesis that $N = N(u)$ is a polynomial implies that $\mathcal{N}(c)$ consists of discrete convolutions. Since $X_{\nu,1}$ is a Banach algebra under discrete convolutions, this implies that for any $r > 0$,

$$\sup_{c \in \overline{B_r(\bar{a})}} \|D_a \mathcal{N}(c)\|_{B(X_{\nu,1})} < \infty.$$

Now, letting $c \in \overline{B_r(\bar{a})}$, using Lemma 4.2 and Lemma 4.3, we get that

$$\begin{aligned}
\|D_a \mathcal{T}(c)\|_{B(X_{\nu,1})} &= \left\| -\frac{h}{2} \mathcal{L}^{-1} \mathbf{K}^{-\tilde{n}} \mathbf{\Lambda} D_a \mathcal{N}(c) \right\|_{B(X_{\nu,1})} \\
&\leq \frac{h}{2} \|\mathcal{L}^{-1} \mathbf{K}^{-\tilde{n}}\|_{B(X_{\nu,1})} \|\mathbf{\Lambda}\|_{B(X_{\nu,1})} \|D_a \mathcal{N}(c)\|_{B(X_{\nu,1})} \\
&\leq h\sigma \|D_a \mathcal{N}(c)\|_{B(X_{\nu,1})} \\
&\leq h\sigma\gamma(r) = Z(r). \tag*{\square}
\end{aligned}$$

Note that the polynomial bound $\gamma(r)$ satisfying (4.4) is problem dependent and will be computed explicitly for each of the PDE models we consider in Section 5.

Remark 4.5 (A priori knowledge about a maximal step size). *Denoting*

$$Z_1 \stackrel{\text{def}}{=} Z(0) = h\sigma\gamma(0) = h\sigma \|D_a \mathcal{N}(\bar{a})\|_{B(X_{\nu,1})}, \tag{72}$$

a necessary condition for the radii polynomial approach to be successful is that $Z_1 < 1$. This is equivalent to require that

$$h < h_{\max} \stackrel{\text{def}}{=} \frac{1}{\sigma \|D_a \mathcal{N}(\bar{a})\|_{B(X_{\nu,1})}}. \tag{73}$$

From this observation, note that the larger $\|\bar{a}\|_{B(X_{\nu,1})}$ is, the larger $\|D_a \mathcal{N}(\bar{a})\|_{B(X_{\nu,1})}$ is (indeed, \mathcal{N} is a polynomial), and therefore smaller the step-size h needs to be for the computer-assisted proof to be successful.

We explain in the section Applications (Section 5) how to make use of the constraint (73) to optimize our code.

4.3 Getting the bounds for the next initial condition

Assume that at a previous time step, we computed $\tilde{a} \in \overline{B_{r_0}(\bar{a})} \stackrel{\text{def}}{=} \{a \in X_{\nu,1} \mid \|a - \bar{a}\|_{X_{\nu,1}} \leq r_0\}$ such that $F(\tilde{a}) = 0$. The initial condition for the next step is then $b = (b_k)_{k \geq k_0}$, where

$$b_k \stackrel{\text{def}}{=} \tilde{a}_k(1) = \tilde{a}_{k,0} + 2 \sum_{j \geq 1} \tilde{a}_{k,j}.$$

Letting

$$\bar{b}_k \stackrel{\text{def}}{=} \bar{a}_{k,0} + 2 \sum_{j \geq 1} \bar{a}_{k,j},$$

then

$$\begin{aligned} \|b - \bar{b}\|_{\ell_\nu^1} &= \delta_{k_0,0} |b_0 - \bar{b}_0| + 2 \sum_{k \geq 1} |b_k - \bar{b}_k| \nu^k \\ &= \delta_{k_0,0} \left| \tilde{a}_{0,0} + 2 \sum_{j \geq 1} \tilde{a}_{0,j} - \bar{a}_{0,0} + 2 \sum_{j \geq 1} \bar{a}_{0,j} \right| + 2 \sum_{k \geq 1} \left| \tilde{a}_{k,0} + 2 \sum_{j \geq 1} \tilde{a}_{k,j} - \bar{a}_{k,0} + 2 \sum_{j \geq 1} \bar{a}_{k,j} \right| \nu^k \\ &\leq \delta_{k_0,0} \left(|\tilde{a}_{0,0} - \bar{a}_{0,0}| + 2 \sum_{j \geq 1} |\tilde{a}_{0,j} - \bar{a}_{0,j}| \right) + 2 \sum_{k \geq 1} |\tilde{a}_{k,0} - \bar{a}_{k,0}| \nu^k + 4 \sum_{k,j \geq 1} |\tilde{a}_{k,j} - \bar{a}_{k,j}| \nu^k \\ &= \sum_{k \geq k_0} \sum_{j \geq 0} |\tilde{a}_{k,j} - \bar{a}_{k,j}| \omega_{k,j} = \|\tilde{a} - \bar{a}\|_{X_{\nu,1}} \leq r_0. \end{aligned}$$

5 Applications

In this section, we apply our approach to four models: Fisher's equation (in Section 5.2), the Kuramoto-Sivashinsky equation (in Section 5.3), the Swift-Hohenberg equation (in Section 5.4) and the Phase-field crystal equation (in Section 5.5).

To apply our approach (and Theorem 2.2) to each of the above PDE models, we compute the radii polynomial $p(r)$ defined in (30). For this we need the bounds Y and $Z = Z(r)$ given by (28) and (29), respectively. In Section 4.1, we introduced the method to obtain the Y bound in full generality in (67). In Section 4.2, recalling (71), we showed that $Z(r) \stackrel{\text{def}}{=} h\sigma\gamma(r)$ satisfied (29) with $\gamma(r)$ satisfying (70). What remains to be done is to obtain explicitly the polynomial bound $\gamma(r)$ for each model, which we do next.

Before doing that, we briefly describe the optimization of the step-size we perform before each computer-assisted proof.

5.1 Procedure for optimizing the step-size before a computer-assisted proof

Recalling Remark 4.5 about the maximal step size, we now present a simple heuristic to optimize the step-size before attempting a computer-assisted proof. Recall the definition of the bound Z_1 in (72), and fix a target value $Z_1^{(\text{target})} < 1$ that we want to achieve for Z_1 and a tolerance tol . In all of the examples below, we chose $Z_1^{(\text{target})} = 0.7$ and $\text{tol} = 0.01$. Fix an initial tentative step-size $h_0 > 0$, and start the procedure.

Compute a solution \bar{a} of $F(\bar{a}, b) = 0$ using an iterative procedure (we use pseudo-Newton $a \mapsto a - \mathcal{L}^{-1}F(a, b)$, which avoids having to compute numerically $DF(\bar{a})$ and $DF(\bar{a})^{-1}$). Make sure that the last Chebyshev coefficients of each Fourier modes $a_k(t)$ are of the order of machine precision ($\approx 10^{-16}$). Then compute (without interval arithmetic) the bound $\sigma = \sigma(h_0)$ given by formula (69). Using (72), compute

$$Z_1 = h\sigma\|D_a\mathcal{N}(\bar{a})\|_{B(X_{\nu,1})},$$

where the bound $\|D_a\mathcal{N}(\bar{a})\|_{B(X_{\nu,1})}$ is easily obtained using Banach algebra estimates (e.g. see the explicit bounds Z_1 (77), (81) and (85) for each model we consider).

- If $Z_1 > Z_1^{(\text{target})}$ and $|Z_1 - Z_1^{(\text{target})}| > \text{tol}$, replace $h_0 \mapsto 0.9h_0$ and start from the beginning.
- If $Z_1 < Z_1^{(\text{target})}$ and $|Z_1 - Z_1^{(\text{target})}| > \text{tol}$, replace $h_0 \mapsto 1.01h_0$ and start from the beginning.
- If $|Z_1 - Z_1^{(\text{target})}| \leq \text{tol}$, then stop the procedure.

Repeat the steps until the wanted tolerance tol is achieved or until you have reached an a priori fixed maximal number of steps.

We are now ready to present some applications.

5.2 Fisher's equation

Fisher's equation is given by

$$u_t = u_{xx} + \alpha u(1 - u), \quad \alpha \in \mathbb{R} \quad (74)$$

and it has applications in mathematical ecology, genetics, and the theory of Brownian motion [32, 33, 34]. We supplement Fisher's equation with even (i.e. $u(t, -x) = u(t, x)$) boundary conditions, plug (4) in (74) and this leads to the following infinite system of ordinary differential equations

$$\frac{d\tilde{a}_k}{dt} = f_k^{(\text{F})}(\tilde{a}) \stackrel{\text{def}}{=} (-k^2 + \alpha)\tilde{a}_k - \alpha(\tilde{a} * \tilde{a})_k, \quad k \geq 0. \quad (75)$$

Recalling (5), we get for Fisher that $k_0 = 0$, $\lambda_k = -k^2 + \alpha$ and $N_k(a) = -\alpha(a^2)_k$. Moreover, $d = 2$ and $n = 0$, and therefore (recalling (14)) $\tilde{n} = d/3 - n = 2/3 > 0$ which implies that assumption (2) holds.

5.2.1 The bound $\gamma(r)$ and h_{\max}

Given any $c \in \overline{B_r(\bar{a})}$ and $h \in \overline{B_1(0)}$, note that $D_a\mathcal{N}(c)h = -2\alpha(c * h)$. Therefore

$$\|D_a\mathcal{N}(c)\|_{B(X_{\nu,1})} \leq \sup_{h \in \overline{B_1(0)}} 2|\alpha|\|c\|_{X_{\nu,1}}\|h\|_{X_{\nu,1}} \leq \gamma(r) \stackrel{\text{def}}{=} 2|\alpha|(\|\bar{a}\|_{X_{\nu,1}} + r).$$

Recalling Lemma 4.4, the polynomial $\gamma(r)$ satisfies (70) and (71), the bound $Z(r)$ for Fisher is given by

$$Z(r) = 2h\sigma|\alpha|\|\bar{a}\|_{X_{\nu,1}} + 2h\sigma|\alpha|r \quad (76)$$

and

$$Z_1 = Z(0) = 2h\sigma|\alpha|\|\bar{a}\|_{X_{\nu,1}}. \quad (77)$$

Hence, when applying the procedure for optimizing the step-size before a computer-assisted proof (see Section 5.1), we have that

$$h < h_{\max} = \frac{1}{2\sigma|\alpha|\|\bar{a}\|_{X_{\nu,1}}}.$$

We fixed the parameter value in Fisher's equation to be $\alpha = 7.1$. At that parameter value, there are 3 unstable eigenvalues (3.1, 6.1 and 7.1). We fixed the initial condition to be $u_0(x) = -0.1 + 0.02 \cos(x) - 0.002 \cos(2x)$. For the whole integration, we fixed the number of Fourier coefficients to be 20. We report the results in Table 1 and in Figure 4.

| Steps | h | # of Cheb. coeff. | \hat{k} | δ | r_0 |
|-------|-------------------------|-------------------|-----------|----------|--------------------------|
| 1 | 8.8589×10^{-2} | 19 | 17 | 15.33 | 5.6644×10^{-12} |
| 2 | 5.8123×10^{-2} | 19 | 19 | 15.33 | 2.6099×10^{-10} |
| 3 | 3.9683×10^{-2} | 18 | 23 | 15.33 | 1.1124×10^{-8} |
| 4 | 2.8929×10^{-2} | 31 | 27 | 15.33 | 4.8552×10^{-7} |
| 5 | 2.1300×10^{-2} | 37 | 31 | 15.33 | 2.0875×10^{-5} |
| 6 | 1.6159×10^{-2} | 41 | 36 | 15.33 | 9.0821×10^{-4} |
| 7 | 1.2258×10^{-2} | 41 | 41 | 15.33 | 4.0301×10^{-2} |

Table 1: Data for the rigorous enclosure of the solution of the Cauchy problem for Fisher’s equation.

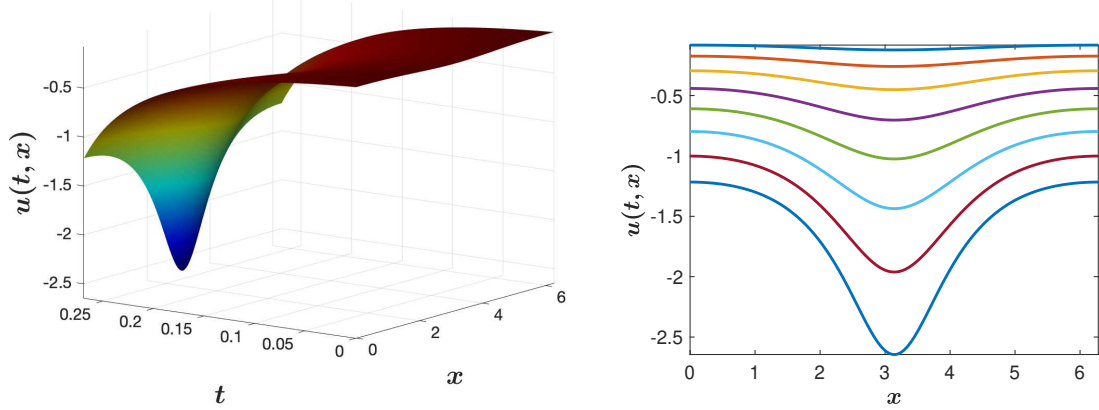


Figure 4: The solution of the Cauchy problem for Fisher with $\alpha = 7.1$ and $u_0(x) = -0.1 + 0.02 \cos(x) - 0.002 \cos(2x)$. Note that u_0 is taken to be approximately in the 3-dimensional unstable manifold of 0. The number of steps is 7 and the total integration time is 0.26504. There are 3 unstable eigenvalues given by $\{3.1, 6.1, 7.1\}$.

5.3 Kuramoto-Sivashinsky equation

Kuramoto-Sivashinsky’s (KS) equation

$$u_t = -\alpha u_{xxxx} - u_{xx} + \partial_x(u^2), \quad \alpha \in \mathbb{R} \quad (78)$$

is popular to analyze weak turbulence or *spatiotemporal chaos* [35, 36, 37, 38]. Considering odd (i.e. $u(t, -x) = -u(t, x)$) boundary conditions and plugging the sine Fourier expansion (3) in (78) leads to the following infinite system of ordinary differential equations

$$\frac{d\tilde{a}_k}{dt} = f_k^{(\text{KS})}(\tilde{a}) \stackrel{\text{def}}{=} (-\alpha k^4 + k^2) \tilde{a}_k - k(\tilde{a} * \tilde{a})_k, \quad k \geq 1. \quad (79)$$

Recalling (5), we get for KS that $k_0 = 1$, $\lambda_k = -\alpha k^4 + k^2$ and $N_k(a) = -(a^2)_k$. Moreover, $d = 4$ and $n = 1$, and therefore (recalling (14)) $\tilde{n} = 4/3 - 1 = 1/3 > 0$ which implies that assumption (2) holds.

5.3.1 The bound $\gamma(r)$ and h_{\max}

Given any $c \in \overline{B_r(\bar{a})}$ and $h \in \overline{B_1(0)}$, $D_a \mathcal{N}(c)h = -2(c * h)$, and hence,

$$\|D_a \mathcal{N}(c)\|_{B(X_{\nu,1})} \leq 2\|c\|_{X_{\nu,1}} \leq \gamma(r) \stackrel{\text{def}}{=} 2(\|\bar{a}\|_{X_{\nu,1}} + r),$$

so that

$$Z(r) = 2h\sigma\|\bar{a}\|_{X_{\nu,1}} + 2h\sigma r \quad (80)$$

and therefore

$$Z_1 = Z(0) = 2h\sigma\|\bar{a}\|_{X_{\nu,1}}. \quad (81)$$

Recall (73) and note that for KS,

$$h < h_{max} = \frac{1}{2\sigma\|\bar{a}\|_{X_{\nu,1}}}.$$

We fixed the parameter value in Kuramoto-Sivashinsky's equation to be $\alpha = 4/150$. At that parameter value, there are 6 unstable eigenvalues: 0.9733, 1.44, 3.5733, 6.84, 8.3333 and 9.1733. We fixed the initial condition to be $u_0(x) = -0.02 \sin(x) - 0.04 \sin(2x)$. For the whole integration, we fixed the number of Fourier coefficients to be 25. We report the results in Table 2 and in Figure 5.

| Steps | h | # of Cheb. coeff. | \hat{k} | δ | r_0 |
|-------|-------------------------|-------------------|-----------|----------|--------------------------|
| 1 | 1.7543×10^{-1} | 22 | 17 | 28.36 | 5.4772×10^{-13} |
| 2 | 1.3308×10^{-1} | 17 | 17 | 22.9 | 3.4531×10^{-11} |
| 3 | 9.7983×10^{-2} | 17 | 17 | 20.27 | 1.9323×10^{-9} |
| 4 | 7.2144×10^{-2} | 16 | 17 | 23.51 | 1.2647×10^{-7} |
| 5 | 2.0376×10^{-2} | 13 | 17 | 147.8 | 5.2398×10^{-5} |
| 6 | 1.8338×10^{-2} | 13 | 17 | 147.8 | 2.3896×10^{-2} |

Table 2: Data for the rigorous enclosure of the solution of the Cauchy problem for KS equation.

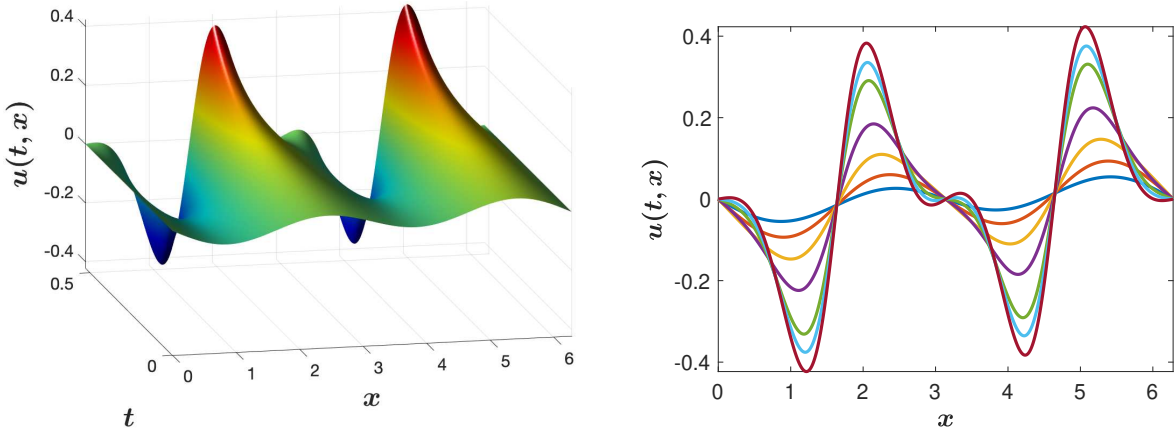


Figure 5: The solution of the Cauchy problem for KS with $\alpha = 4/150$ and $u_0(x) = -0.02 \sin(x) - 0.04 \sin(2x)$. The number of steps is 6 and the total integration time is 0.51734. There are 6 unstable eigenvalues which are given by $\{0.9733, 1.44, 3.5733, 6.84, 8.3333, 9.1733\}$.

5.4 Swift-Hohenberg equation

Swift-Hohenberg's (SH) equation

$$u_t = (\alpha - 1)u - 2u_{xx} - u_{xxxx} - u^3, \quad \alpha \in \mathbb{R} \quad (82)$$

is used as a model for pattern formation due to a finite wavelength instability, such as in Rayleigh–Bénard convection [39, 40]. Considering even boundary conditions leads (via the cosine Fourier expansion (4) plugged in (82)) to

$$\frac{d\tilde{a}_k}{dt} = f_k^{(\text{SH})}(\tilde{a}) \stackrel{\text{def}}{=} (-k^4 + 2k^2 + \alpha - 1)\tilde{a}_k - (\tilde{a} * \tilde{a} * \tilde{a})_k, \quad k \geq 0. \quad (83)$$

Recalling (5), we get for SH that $k_0 = 0$, $\lambda_k = -k^4 + 2k^2 + \alpha - 1$ and $N_k(a) = -(a^3)_k$. Moreover, $d = 4$ and $n = 0$, and therefore (recalling (14)) $\tilde{n} = 4/3 > 0$ which implies that assumption (2) holds.

5.4.1 The bound $\gamma(r)$ and h_{\max}

Given any $c \in \overline{B_r(\bar{a})}$ and $h \in \overline{B_1(0)}$, $D_a \mathcal{N}(c)h = -3c_1^2 * c_2$, and hence

$$\|D_a \mathcal{N}(c)\|_{B(X_{\nu,1})} \leq \gamma(r) \stackrel{\text{def}}{=} 3(\|\bar{a}\|_{X_{\nu,1}} + r)^2.$$

We therefore set

$$Z(r) = 3h\sigma\|\bar{a}\|_{X_{\nu,1}}^2 + 6h\sigma\|\bar{a}\|_{X_{\nu,1}}r + 3h\sigma r^2 \quad (84)$$

and

$$Z_1 = Z(0) = 3h\sigma\|\bar{a}\|_{X_{\nu,1}}^2. \quad (85)$$

Recall (73) and note that for SH,

$$h < h_{\max} = \frac{1}{3\sigma\|\bar{a}\|_{X_{\nu,1}}^2}.$$

We consider $\alpha = 8.1$. At that parameter value, there are 2 unstable eigenvalues: 7.1 and 8.1. Fix the initial condition to be $u_0(x) = 0.02 \cos(x)$ which is roughly is the unstable manifold of $u \equiv 0$. We fix $\hat{k} = 5$, which fixes the number of blocks \mathcal{L}_k ($k = k_0 = 0, \dots, 5$), that we invert using the computer-assisted approach of Section 3.1. For the whole integration, we fixed the number of Fourier coefficients to be 15. We report the results in Table 3 and in Figure 6.

| Steps | h | # of Cheb. coeff. | \hat{k} | δ | r_0 |
|-------|-------------------------|-------------------|-----------|----------|--------------------------|
| 1 | 3.1683×10^{-1} | 39 | 5 | 15.33 | 2.1523×10^{-12} |
| 2 | 1.3559×10^{-1} | 20 | 5 | 15.33 | 1.0701×10^{-10} |
| 3 | 6.7484×10^{-2} | 18 | 5 | 15.33 | 4.8450×10^{-9} |
| 4 | 4.1881×10^{-2} | 26 | 5 | 15.33 | 2.1416×10^{-7} |
| 5 | 3.0532×10^{-2} | 41 | 6 | 15.33 | 9.4355×10^{-6} |
| 6 | 2.3863×10^{-2} | 41 | 6 | 15.33 | 4.0225×10^{-4} |
| 7 | 2.0114×10^{-2} | 41 | 6 | 15.33 | 1.7784×10^{-2} |

Table 3: Data for the rigorous enclosure of the solution of the Cauchy problem for SH equation.

We report some results in Figure 6.

5.5 Phase-field crystal equation

The phase-field crystal (PFC) equation is given by

$$u_t = u_{xxxxxx} + 2u_{xxxx} + (1 - \alpha)u_{xx} + \partial_x^2(u^3), \quad \alpha \in \mathbb{R} \quad (86)$$

and was recently introduced in [41] as a new model of crystal growth that describes the phenomena on atomic length and diffusive time scales. We refer to the review article [42] for the basic concepts and applications of the PFC model.

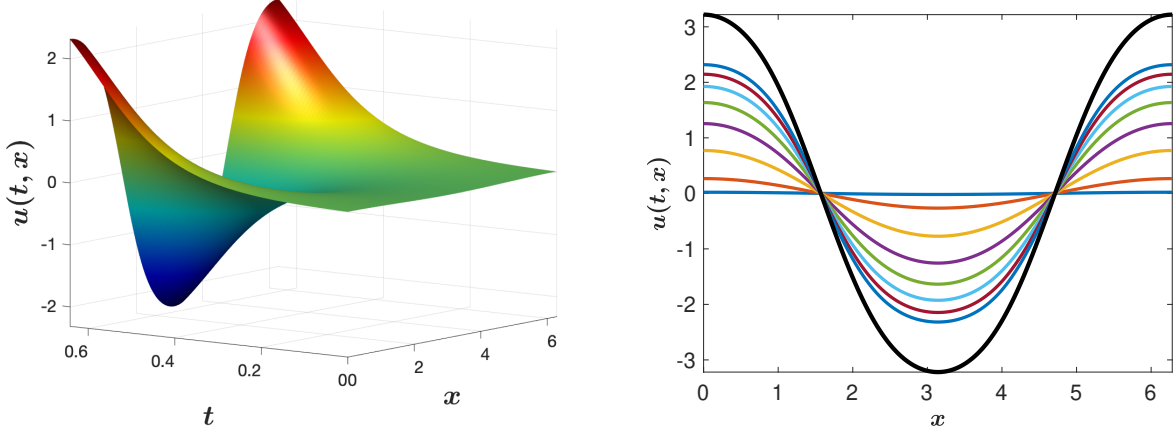


Figure 6: The solution of the Cauchy problem for the Swift-Hohenberg equation with $\alpha = 8.1$ and $u_0(x) = 0.02 \cos(x)$, which is roughly is the unstable manifold of $u \equiv 0$. The number of steps is 7 and the total integration time is 0.63629. In thick black, we portrait the graph of a steady states of (82), which shows that we get a large part of a connecting orbit between 0 and the nontrivial steady states. Note that there are two unstable eigenvalues: 7.1 and 8.1.

We supplement (86) with even BCs, plug the cosine Fourier expansion (4) in (86) and obtain the system

$$\frac{d\tilde{a}_k}{dt} = f_k^{(\text{PFC})}(\tilde{a}) \stackrel{\text{def}}{=} (-k^6 + 2k^4 + (\alpha - 1)k^2) \tilde{a}_k - k^2(\tilde{a} * \tilde{a} * \tilde{a})_k, \quad k \geq 1. \quad (87)$$

where the coefficient $a_0(t)$ is fixed to a given constant $\bar{\psi}$. This amounts to imposing that the total phase constraint $\frac{1}{2\pi} \int_0^{2\pi} u(t, x) dx = \bar{\psi}$ holds at all times.

Recalling (5), we get for PFC that $k_0 = 1$, $\lambda_k = -k^6 + 2k^4 + (\alpha - 1)k^2$ and $N_k(a) = -(a^3)_k$. Moreover, $d = 6$ and $n = 2$, and therefore (recalling (14)) $\tilde{n} = 6/3 - 2 = 0 \geq 0$ which implies that assumption (2) holds.

Note that the polynomial bound $\gamma(r)$ and the step size h_{\max} are the same as for the Swift-Hohenberg equation.

We fixed the parameter value in the PFC equation to be $\alpha = 40$. At that parameter value, there are 2 (large) unstable eigenvalues (40 and 124), which means that the problem is stiff. We fixed the initial condition to be $u_0(x) = -0.05 \cos(2x) + 0.01 \cos(3x)$. For the whole integration, we fixed the number of Fourier coefficients to be 20. We report the results in Table 4 and in Figure 7.

| Steps | h | # of Cheb. coeff. | \hat{k} | δ | r_0 |
|-------|-------------------------|-------------------|-----------|----------|--------------------------|
| 1 | 1.9480×10^{-2} | 242 | 5 | 26.35 | 2.1936×10^{-11} |
| 2 | 6.1129×10^{-3} | 51 | 5 | 22.98 | 1.2241×10^{-9} |
| 3 | 2.1315×10^{-3} | 51 | 5 | 34.22 | 8.3938×10^{-8} |
| 4 | 7.1712×10^{-4} | 33 | 6 | 110.48 | 2.5982×10^{-5} |
| 5 | 6.2277×10^{-4} | 12 | 6 | 110.48 | 8.2604×10^{-3} |

Table 4: Data for the rigorous enclosure of the solution of the Cauchy problem for the PFC model.

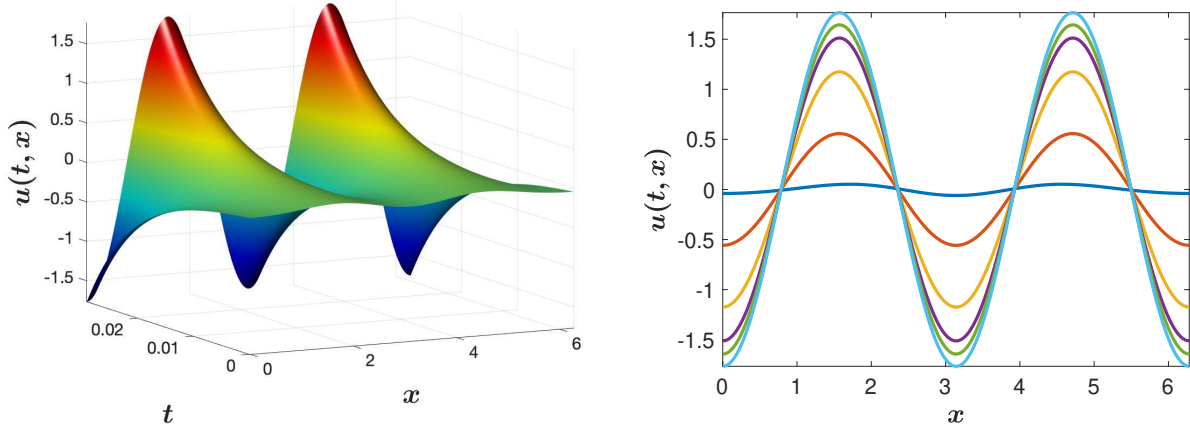


Figure 7: The solution of the Cauchy problem for the PFC equation with $\alpha = 40$ and $u_0(x) = -0.05 \cos(2x) + 0.01 \cos(3x)$. The number of steps is 5 and the total integration time is 0.029064. There are 2 unstable eigenvalues given by $\{40, 124\}$.

6 Future directions

There are many future research directions and open problems related to the described method that we will pursue in our future work. Major research efforts will be devoted to making our approach applicable for performing computer-assisted proofs in dynamics that require validated forward integration, like the existence of periodic and connecting orbits. To achieve this ultimate goal several improvements will be introduced. First, to deal with longer orbits (i.e. larger h) and larger solutions $\mathcal{L} = DF(\bar{a})$ should be considered instead of $\mathcal{L} = DF(0)$ when computing an approximate inverse for a Newton-like operator. Second, an effective way of fighting the wrapping effect needs to be employed (see Remark 4.1). Virtually all forward integration schemes suffer the issue when the error resulting from a single step of forward integration is being accumulated in a multiplicative way and leads to blow-up of bounds after a finite time. A promising simple solution to this issue in the context of our method is to employ a multi-step forward integration operator instead of the single-step one and consider an algebraic system of equations determining the coefficients of a solution over a longer time interval.

A very important research direction is to generalize our technique to other important PDEs that are beyond scope of the present implementation, including Burgers, Navier-Stokes, Cahn-Hilliard and Ohta-Kawasaki model. After this step is succeeded a thorough comparison with the mentioned in the introduction alternative approaches will be performed. Generalizing this approach to PDEs defined on higher dimensional domains (allowing a Fourier expansion in space) is also an interesting direction. Another related research directions that we will pursue are purely technical, related to improving the inverse operator upper norm bounds and attempt to decrease the sensitivity of the bounds on time-interval length h .

7 Acknowledgements

The project was initiated at Semester Program Workshop ‘‘Computation in Dynamics’’ organized at the Institute for Computational and Experimental Research in Mathematics (ICERM) in 2016. JC was partially supported by NAWA Polish Returns grant PPN/PPO/2018/1/00029. JPL was supported by an NSERC Discovery Grant.

References

- [1] Piotr Zgliczyński. Rigorous numerics for dissipative partial differential equations. II. Periodic orbit for the Kuramoto-Sivashinsky PDE—a computer-assisted proof. *Found. Comput. Math.*, 4(2):157–185, 2004.
- [2] Piotr Zgliczyński. Rigorous numerics for dissipative PDEs III. An effective algorithm for rigorous integration of dissipative PDEs. *Topol. Methods Nonlinear Anal.*, 36(2):197–262, 2010.
- [3] Daniel Wilczak and Piotr Zgliczyński. A geometric method for infinite-dimensional chaos: symbolic dynamics for the Kuramoto-Sivashinsky PDE on the line. *J. Differential Equations*, 269(10):8509–8548, 2020.
- [4] Jacek Cyranka. Efficient and generic algorithm for rigorous integration forward in time of dPDEs: Part I. *J. Sci. Comput.*, 59(1):28–52, 2014.
- [5] Jacek Cyranka and Thomas Wanner. Computer-assisted proof of heteroclinic connections in the one-dimensional Ohta-Kawasaki Model. *SIAM J. Appl. Dyn. Syst.*, 17(1):694–731, 2018.
- [6] Jacek Cyranka. Existence of globally attracting fixed points of viscous burgers equation with constant forcing. a computer assisted proof. *Topol. Methods Nonlinear Anal.*, 45(2):655–697, 2015.
- [7] Jacek Cyranka and Piotr Zgliczyński. Existence of Globally Attracting Solutions for One-Dimensional Viscous Burgers Equation with Nonautonomous Forcing—A Computer Assisted Proof. *SIAM Journal on Applied Dynamical Systems*, 14(2):787–821, 2015.
- [8] Gianni Arioli and Hans Koch. Integration of dissipative partial differential equations: a case study. *SIAM J. Appl. Dyn. Syst.*, 9(3):1119–1133, 2010.
- [9] Makoto Mizuguchi, Akitoshi Takayasu, Takayuki Kubo, and Shin’ichi Oishi. A method of verified computations for solutions to semilinear parabolic equations using semigroup theory. *SIAM J. Numer. Anal.*, 55(2):980–1001, 2017.
- [10] Akitoshi Takayasu, Makoto Mizuguchi, Takayuki Kubo, and Shin’ichi Oishi. Accurate method of verified computing for solutions of semilinear heat equations. *Reliab. Comput.*, 25:74–99, 2017.
- [11] Akitoshi Takayasu, Jean-Philippe Lessard, Jonathan Jaquette, and Hisashi Okamoto. Rigorous numerics for nonlinear heat equations in the complex plane of time. Preprint, 2019.
- [12] Jonathan Jaquette, Jean-Philippe Lessard, and Akitoshi Takayasu. Global dynamics in nonconservative nonlinear Schrödinger equations. Preprint, 2020.
- [13] Kouji Hashimoto, Takehiko Kinoshita, and Mitsuhiro Nakao. Numerical verification of solutions for nonlinear parabolic problems. *Numerical Functional Analysis and Optimization*, 41:1–20, 06 2020.
- [14] Takuma Kimura, Teruya Minamoto, and Mitsuhiro Nakao. Constructive error estimates for full discrete approximation of periodic solution for heat equation. *Journal of Computational and Applied Mathematics*, 368:112510, 09 2019.
- [15] Mitsuhiro Nakao, Michael Plum, and Yoshitaka Watanabe. *Numerical Verification Methods and Computer-Assisted Proofs for Partial Differential Equations*. Springer Singapore, 2019.
- [16] Jordi-Lluís Figueras, Marcio Gameiro, Jean-Philippe Lessard, and Rafael de la Llave. A framework for the numerical computation and a posteriori verification of invariant objects of evolution equations. *SIAM J. Appl. Dyn. Syst.*, 16(2):1070–1088, 2017.

- [17] Marcio Gameiro and Jean-Philippe Lessard. A posteriori verification of invariant objects of evolution equations: periodic orbits in the Kuramoto-Sivashinsky PDE. *SIAM J. Appl. Dyn. Syst.*, 16(1):687–728, 2017.
- [18] Jordi-Lluís Figueras and Rafael de la Llave. Numerical computations and computer assisted proofs of periodic orbits of the Kuramoto-Sivashinsky equation. *SIAM J. Appl. Dyn. Syst.*, 16(2):834–852, 2017.
- [19] Jan Bouwe van den Berg, Maxime Breden, Jean-Philippe Lessard, and Lennaert van Veen. Spontaneous periodic orbits in the navier-stokes flow. Preprint, 2020.
- [20] Jacek Cyranka and Piotr Bogusław Mucha. A construction of two different solutions to an elliptic system. *Journal of Mathematical Analysis and Applications*, 465(1):500 – 530, 2018.
- [21] Maxime Breden, Laurent Desvillettes, and Jean-Philippe Lessard. Rigorous numerics for nonlinear operators with tridiagonal dominant linear parts. *Discrete and Continuous Dynamical Systems - Series A*, 35(10):4765–4789, 2015.
- [22] Jean-Philippe Lessard and Christian Reinhardt. Rigorous Numerics for Nonlinear Differential Equations Using Chebyshev Series. *SIAM J. Numer. Anal.*, 52(1):1–22, 2014.
- [23] Allan Hungria, Jean-Philippe Lessard, and J. D. Mireles James. Rigorous numerics for analytic solutions of differential equations: the radii polynomial approach. *Math. Comp.*, 85(299):1427–1459, 2016.
- [24] Fuzhen Zhang. *The Schur Complement and its Applications*, volume 4 of *Numerical Methods and Algorithms*. Springer, New York, 2005.
- [25] Kouta Sekine, Mitsuhiro Nakao, and Shin’ichi Oishi. A new formulation using the schur complement for the numerical existence proof of solutions to elliptic problems: without direct estimation for an inverse of the linearized operator. *Numerische Mathematik*, 146:1–20, 12 2020.
- [26] Wolfram Research, Inc. Mathematica, Version 12.1. Champaign, IL, 2020.
- [27] Winifred J. Sherman, Jack; Morrison. Adjustment of an inverse matrix corresponding to changes in the elements of a given column or a given row of the original matrix (abstract). *Annals of Mathematical Statistics*, 20:621, 1949.
- [28] Winifred J. Sherman, Jack; Morrison. Adjustment of an inverse matrix corresponding to a change in one element of a given matrix. *Annals of Mathematical Statistics*, 21(1):124–127, 1950.
- [29] Max A. Woodbury. *Inverting modified matrices*. Number 42 in Statistical Research Group, Memo. Rep. Princeton University, Princeton, N. J., 1950.
- [30] Max A. Woodbury. *The Stability of Out-Input Matrices*. Chicago, Ill., 1949.
- [31] Maurice S. Bartlett. An inverse matrix adjustment arising in discriminant analysis. *Annals of Mathematical Statistics*, 22(1):107–111, 1951.
- [32] Peter Grindrod. *The theory and applications of reaction-diffusion equations*. Oxford Applied Mathematics and Computing Science Series. The Clarendon Press, Oxford University Press, New York, second edition, 1996. Patterns and waves.
- [33] Mark J. Ablowitz and Anthony Zeppetella. Explicit solutions of Fisher’s equation for a special wave speed. *Bull. Math. Biol.*, 41(6):835–840, 1979.
- [34] H. P. McKean. Application of Brownian motion to the equation of Kolmogorov-Petrovskii-Piskunov. *Comm. Pure Appl. Math.*, 28(3):323–331, 1975.

- [35] Y. Kuramoto and T. Tsuzuki. Persistent propagation of concentration waves in dissipative media far from thermal equilibrium. *Prog. Theor. Phys.*, 55(365), 1976.
- [36] G. I. Sivashinsky. Nonlinear analysis of hydrodynamic instability in laminar flames. I. Derivation of basic equations. *Acta Astronaut.*, 4(11-12):1177–1206, 1977.
- [37] F. Christiansen, P. Cvitanović, and V. Putkaradze. Spatiotemporal chaos in terms of unstable recurrent patterns. *Nonlinearity*, 10(1):55–70, 1997.
- [38] Yueheng Lan and Predrag Cvitanović. Unstable recurrent patterns in Kuramoto-Sivashinsky dynamics. *Phys. Rev. E (3)*, 78(2):026208, 12, 2008.
- [39] J.B. Swift and P.C. Hohenberg. Hydrodynamic fluctuations at the convective instability. *Phys. Rev. A*, 15(1), 1977.
- [40] M. C. Cross and P. C. Hohenberg. Pattern formation outside of equilibrium. *Rev. Modern Phys.*, 65(3):851–1112, 1993.
- [41] K. R. Elder, Mark Katakowski, Mikko Haataja, and Martin Grant. Modeling elasticity in crystal growth. *Phys. Rev. Lett.*, 88(24):245701, 2002.
- [42] Heike Emmericha, Hartmut Lowenb, Raphael Wittkowskib, Thomas Gruhna, Gyula I. Tothc, Gyorgy Tegzec, and Laszlo Granasy. Phase-field-crystal models for condensed matter dynamics on atomic length and diffusive time scales: an overview. *Advances in Physics*, 61(6):665–743, 2012.

A Computer-Assisted Proof of Theorem 3.17

Here we demonstrate a computer assisted proof of our main result for the Kuramoto-Sivashinsky equation (Theorem 3.17). The proofs for other considered PDEs (Theorem 3.18, 3.20, 3.19) are analogous to the presented proof, and we do not present them in detail.

Let us denote $\mu = \mu_k$. The fundamental idea behind the proof is to apply in practice Theorem 3.11 and Lemma 3.13, which provide explicit recursive formulas for all values in T_k^{-1} . By summing up and unveiling the recursion in the formulas we obtain an explicit formula for the ℓ^1 norm of each column of $k^{d/3} \cdot T_k^{-1}$. Namely, the ℓ^1 norm of each column of $k^{d/3} \cdot T_k^{-1}$ is expressed by the formula

$$k^{d/3} |\tilde{I}_{col(c)}| + |\tilde{I}_{2c}| \mu k^{d/3} \left[(\hat{a}_{n-1} + a_{n-1}) + \mu \hat{a}_{n-1} (\hat{a}_{n-2} + a_{n-2}) + \mu^2 \hat{a}_{n-1} \hat{a}_{n-2} (\hat{a}_{n-3} + a_{n-3}) + \dots + \mu^{n-2} \prod_{l=1}^{n-2} \hat{a}_{n-l} (\hat{a}_1 + a_1) \right],$$

where $c = 1$ or 2 , \tilde{I} is the diagonal block (48) corresponding to the considered column. We denote

$$\alpha_n \stackrel{\text{def}}{=} |\tilde{I}_{2c}| \mu k^{d/3} \left[(\hat{a}_{n-1} + a_{n-1}) + \mu \hat{a}_{n-1} (\hat{a}_{n-2} + a_{n-2}) + \mu^2 \hat{a}_{n-1} \hat{a}_{n-2} (\hat{a}_{n-3} + a_{n-3}) + \dots + \mu^{n-2} \prod_{l=1}^{n-2} \hat{a}_{n-l} (\hat{a}_1 + a_1) \right].$$

We define recursively the sequence, which will be easily estimated in what follows

$$\alpha_n \stackrel{\text{def}}{=} |\tilde{I}_{2c}| \mu \hat{a}_{n-1} \alpha_{n-1}, \quad (88a)$$

$$\alpha_{n-1} \stackrel{\text{def}}{=} k^{d/3} \left(1 + \frac{a_{n-1}}{\hat{a}_{n-1}} \right) + \mu \hat{a}_{n-2} \alpha_{n-2}, \quad (88b)$$

$$\alpha_{n-2} \stackrel{\text{def}}{=} k^{d/3} \left(1 + \frac{a_{n-2}}{\hat{a}_{n-2}} \right) + \mu \hat{a}_{n-3} \alpha_{n-3}, \quad (88c)$$

$$\dots, \quad (88d)$$

$$\alpha_1 \stackrel{\text{def}}{=} k^{d/3} \left(1 + \frac{a_1}{\hat{a}_1} \right). \quad (88e)$$

We study finite dimensional matrix $k^{d/3} \cdot T_k^{-1}$ of size equal to $N = 2\mu$ (observe that it is dependent on μ), for the remainder we have the tail bound from Theorem 3.15. The proof consists of two steps which proceed differently depending on the magnitude of μ .

First Step. Proof for Sufficiently Large $\mu \geq \bar{\mu}$. Symbolic Computation. For sufficiently large values of μ we proceed as follows. Assume (without loosing generality) that μ is an integer. Let us consider the worst case when $n = \mu$ (corresponding to the first two columns of $k^{d/3} \cdot T_k^{-1}$), we will use the bound

$$\left\| k^{d/3} \cdot T_k^{-1} \right\|_{B(\ell^1)} \leq k^{d/3} |\tilde{I}_{col(c)}| + \alpha_\mu + \left\| T_{row(2\lfloor \mu_k \rfloor + 1: N)}^{-1} \right\|_{B(\ell^1)}, \quad (89)$$

where $c = 1$ or $c = 2$, and \tilde{I} is the upper-left corner 2×2 matrix, α_μ is the recursively computed number (88) bounding ℓ^1 norm of the finite column of size 2μ but the first two its elements, and $\left\| T_{row(2\lfloor \mu_k \rfloor + 1: N)}^{-1} \right\|_{B(\ell^1)}$ is the tail bound from Lemma 3.15.

We present below the details of our computer-assisted proof based on symbolic computations performed using the Mathematica scripts.

We use the following bound for the diagonal blocks \tilde{I}

$$\begin{aligned} |\tilde{I}_{21}| &= \frac{\mu}{(d_{N-2n+1} + \mu^2 b_{\frac{N-2n}{2}})(d_{N-2n+2} + \mu^2 a_{n-1}) + \mu^2} < \frac{1}{\mu}, \\ |\tilde{I}_{22}| &= \frac{d_{N-2n+1} + \mu^2 b_{\frac{N-2n}{2}}}{(d_{N-2n+1} + \mu^2 b_{\frac{N-2n}{2}})(d_{N-2n+2} + \mu^2 a_{n-1}) + \mu^2} \leq \frac{1}{\mu}. \end{aligned} \quad (90)$$

We use the following trivial lower bound for a_1

$$a_1 = \frac{d_N}{d_{N-1}d_N + \mu_k^2} \geq \frac{2\mu}{5\mu^2} \geq \frac{2}{5\mu}. \quad (91)$$

And using the upper bound $a_{j-1} \leq \frac{\sqrt{2}}{\mu}$ from Lemma 3.7, we obtain the following upper bound for a_j

$$a_j \leq \frac{d_{N-2j+2} + \sqrt{2}\mu}{d_{N-2j+2}d_{N-2j+1} + a_1 d_{N-2j+1}\mu^2 + \mu^2} \leq \frac{d_{N-2j+2} + \sqrt{2}\mu}{d_{N-2j+2}d_{N-2j+1} + 2d_{N-2j+1}\mu/5 + \mu^2} = A_j.$$

All the quotients appearing in (88) we overestimate by

$$\frac{a_j}{\hat{a}_j} = \frac{d_{N-2j+2} + a_{j-1}\mu^2}{\mu} \leq \frac{d_{N-2j+2} + a_j\mu^2}{\mu} \leq \frac{d_{N-2j+2} + A_j\mu^2}{\mu}, \quad (92)$$

for $j = 2, \dots, n$, α_j depends on α_{j-1} in the following way, where in the formula for \hat{a}_j we plug in $a_{j-1} = \frac{2}{5\mu}$, due to the monotonicity property from Lemma 3.6, the bound from Lemma 3.7, and the upper bound for the quotients (92).

$$\alpha_j = k^{d/3} \left(1 + \frac{d_{N-2j+2} + A_j \mu^2}{\mu} \right) + \frac{\mu}{d_{N-2j+1} d_{N-2j+2} + 2d_{N-2j+1} \mu/5 + \mu^2} \mu \alpha_{j-1}.$$

Assume that

$$\alpha_{j-1} \leq C_{j-1} \mu, \quad (93)$$

for some

$$C_{j-1} \geq 1,$$

then

$$\alpha_j \leq k^{d/3} \left(1 + \frac{d_{N-2j+2} + A_j \mu^2}{\mu} \right) + \frac{\mu}{d_{N-2j+1} d_{N-2j+2} + 2d_{N-2j+1} \mu/5 + \mu^2} \cdot C_{j-1} \mu^2, \quad (94)$$

pulling out μ

$$\alpha_j \leq \overbrace{\left[\frac{K}{\mu^{2/3}} \left(1 + \frac{d_{N-2j+2} + A_j \mu^2}{\mu} \right) + \frac{\mu^2}{d_{N-2j+1} d_{N-2j+2} + 2d_{N-2j+1} \mu/5 + \mu^2} \cdot C_{j-1} \right]}^{C_j} \mu. \quad (95)$$

We compute the bound K such that

$$\frac{k^{d/3}}{\mu} \leq \frac{K}{\mu^{2/3}},$$

where K is a constant such that $k^{d/3} \leq K \mu^{1/3}$, which always exists as d is the order of the maximal derivative in the linear part of the equation under study. Observing that $\mu_k = \frac{h}{2} \lambda_k$, where λ_k are the eigenvalues of the linear part, constant K inversely depend on integration interval h , and a possible constant in front of the dominant order term of the linear part. In fact, the proof is the hardest in the Kuramoto-Sivashinsky case partially due to αk^4 term in the linear part. Also, note that once constant K is chosen such that $k^{d/3} \leq K \mu^{1/3}$ is satisfied for a given \tilde{h} , the bound obviously hold also for values $h > \tilde{h}$.

Observe that from our assumption that $C_{j-1} \geq 1$ it follows that

$$\alpha_j \leq C_j \mu \leq \left[\frac{K}{\mu^{2/3}} \left(1 + \frac{d_{N-2j+2} + A_j \mu^2}{\mu} \right) + \frac{\mu^2}{d_{N-2j+1} d_{N-2j+2} + 2d_{N-2j+1} \mu/5 + \mu^2} \right] C_{j-1} \mu. \quad (96)$$

Let us now investigate asymptotic properties of α_j . Define

$$f(x) \stackrel{\text{def}}{=} g(x) + h(x),$$

$$g(x) = \frac{K}{\mu^{2/3}} \left(1 + \frac{2(2\mu - 2x + 2) + \frac{2(2\mu - 2x + 2)\mu^2 + \sqrt{2}\mu^3}{4(2\mu - 2x + 2)(2\mu - 2x + 1) + 4(2\mu - 2x + 1)\mu/5 + \mu^2}}{\mu} \right),$$

$$h(x) = \frac{\mu^2}{4(2\mu - 2x + 1)(2\mu - 2x + 2) + 4(2\mu - 2x + 1)\mu/5 + \mu^2}.$$

Therefore, for $j = 3, \dots, \mu - 1$ under assumption that all $C_j \geq 1$ it holds that

$$\alpha_j \leq f(j) C_{j-1} \mu, \text{ and } \alpha_j \leq f(j) f(j-1) \cdots f(2) C_1 \mu, \quad (97)$$

We use the substitution $y = \mu - x$,

$$f(\mu - x) = \hat{f}(y) = \hat{g}(y) + \hat{h}(y) \quad (98)$$

(97) becomes (recall that $n = \mu$)

$$\alpha_j \leq \hat{f}(\mu - j)C_{j-1}\mu, \text{ and } \alpha_j \leq \hat{f}(\mu - j)\hat{f}(\mu - j + 1) \cdots \hat{f}(\mu - 2)C_1\mu,$$

Observe that this estimate is under assumption that all $C_j \geq 1$, hence any $\hat{f}(\mu - j) < 1$ is replaced by 1 in the above estimate. Using symbolic computations in Mathematica notebooks *main_bound_KS_1.nb*, *main_bound_KS_2.nb*, *main_bound_KS_3.nb*, we show that for sufficiently large values of μ , \hat{f} satisfies the several properties listed below.

Depending on the considered lower bound for the parameter $\alpha \cdot h$ in Theorem 3.17, we pick a constant $\tilde{C} \in (0, 1)$ accordingly:

Case 1, $\tilde{C} = 1.31$;

Case 2, $\tilde{C} = 1.5$;

Case 3, $\tilde{C} = 2.193$.

\tilde{C} can be chosen arbitrarily here, and the intuition behind the particular choice of \tilde{C} is that the smaller \tilde{C} is, the lower the resulting α_j upper bound will be, but also the larger the lower bound $\bar{\mu}$ for μ values.

We show that for $\mu > \bar{\mu}$ it holds that

1. $\hat{f}(y)$ is less than 1 for all $y \geq \tilde{C}\mu^{1/2}$,
2. $\hat{f}(y)$ is decreasing for all $y \in [0, \tilde{C}\mu^{1/2}]$.

Observe that from 1. and 2. it follows that the global maximum of $\hat{f}(y)$ is attained at $y = 0$.

Also, using facts 1. and 2. listed above we compute the global maximum of $\hat{f}(y)$, and denote it by M (computed explicitly using symbolic computation).

Our goal now is to estimate

$$\alpha_{\mu-1} \leq \hat{f}(1)\hat{f}(2) \cdots \hat{f}(\mu-1)C_1\mu. \quad (99)$$

From 1., 2. above it follows that $\hat{f}(y) \leq 1$ for any $y \geq \tilde{C}\mu^{1/2}$ and

$$\hat{f}(y) \leq M \text{ for any } y < \tilde{C}\mu^{1/2}.$$

Therefore from (99) we obtain

$$\alpha_{\mu-1} \leq \underbrace{M \cdots M}_{\tilde{C}\mu^{1/2} \text{ times}} \cdot C_1\mu \leq M^{\tilde{C}\mu^{1/2}} \cdot C_1\mu = C(\mu)\mu.$$

For $\mu > \bar{\mu}$ it holds that

$$\alpha_{\mu-1} \leq C(\mu)\mu,$$

and $C(\mu)$ is decreasing ($M^{\tilde{C}\mu^{1/2}}$ converges with $\mu \rightarrow \infty$ and is decreasing due to the highest order of μ in M is smaller than $1/2$). Plugging in (88a) and using the bound (90) we have that

$$\alpha_\mu \leq \hat{a}_{\mu-1}C(\mu)\mu \leq C(\mu) \frac{\mu^2}{48 + 12\mu/5 + \mu^2} \leq C(\bar{\mu}) \frac{\bar{\mu}^2}{48 + 12\bar{\mu}/5 + \bar{\mu}^2},$$

we plugin the explicit value for $\hat{a}_{\mu-1}$, see Def. 3.5, and use the lower bound for a_1 (91). Refer to the Mathematica script for computation of explicit values of $C(\bar{\mu})$.

Therefore, after adding the uniform tail bound from Theorem 3.15 we obtain the final bound for (89)

$$\|k^{d/3} \cdot T_k^{-1}\|_{B(\ell^1)} \leq k^{d/3} |\tilde{I}_{col(1)}| + \frac{C(\mu)\mu^2}{48 + 12\mu/5 + \mu^2} + \frac{k^{d/3}}{\mu} \leq K\bar{\mu}^{1/3} \frac{4 + (1 + \sqrt{2})\bar{\mu}}{\bar{\mu}^2 + 4\bar{\mu}/5 + 8} + \frac{C(\bar{\mu})\bar{\mu}^2}{48 + 12\bar{\mu}/5 + \bar{\mu}^2} + \frac{K}{\bar{\mu}^{2/3}}$$

for all $\mu > \bar{\mu}$, where $\tilde{I} = \begin{bmatrix} d_1 & \mu_k \\ -\mu_k & d_2 + \mu^2 a_{\mu-1} \end{bmatrix}^{-1}$, $|\tilde{I}_{col(1)}| = \frac{4+\sqrt{2}\mu}{\mu^2+4\mu/5+8} + \frac{\mu}{\mu^2+4\mu/5+8}$, and additionally using the bound $k^{d/3} \leq K\mu^{1/3}$ (which appeared earlier).

Observe that the final estimate that we obtain is true asymptotically for $\mu > \bar{\mu}$. Hence the final step of the proof is for μ values within range $[30000, \bar{\mu}]$, as we precompute for values $\mu < 30000$.

Second Step. Proof for μ values within range $[30000, \bar{\mu}]$ For values of μ within range $[30000, \bar{\mu}]$ we perform an explicit computation of a upper bound for $\{\alpha_j\}$ recursive sequence elements using (95). In fact, the obtained bound in the asymptotic proof $\bar{\mu}$ is $1.5 \cdot 10^6$, and in the hardest case over $2 \cdot 10^6$. Refer to Fig. 8 for an example plot presenting the upper bound as a function of μ obtained in the finite range. The computation of an upper bound for the recursive sequence is performed by a C++ program utilizing interval arithmetic attached in supplementary materials. The resulting bounds are stored in .csv files found within *norm_databases_used_in_proofs* sub-directories depending on the value of K constant (*database2_K9.12*, *database2_K10.44*, *database2_K16.57*). The final bound for $\|k^{d/3} \cdot T_k^{-1}\|_{B(\ell^1)}$ is the maximum of values obtained for the finite range of μ values and the asymptotic bound (usually equal to the asymptotic bound).

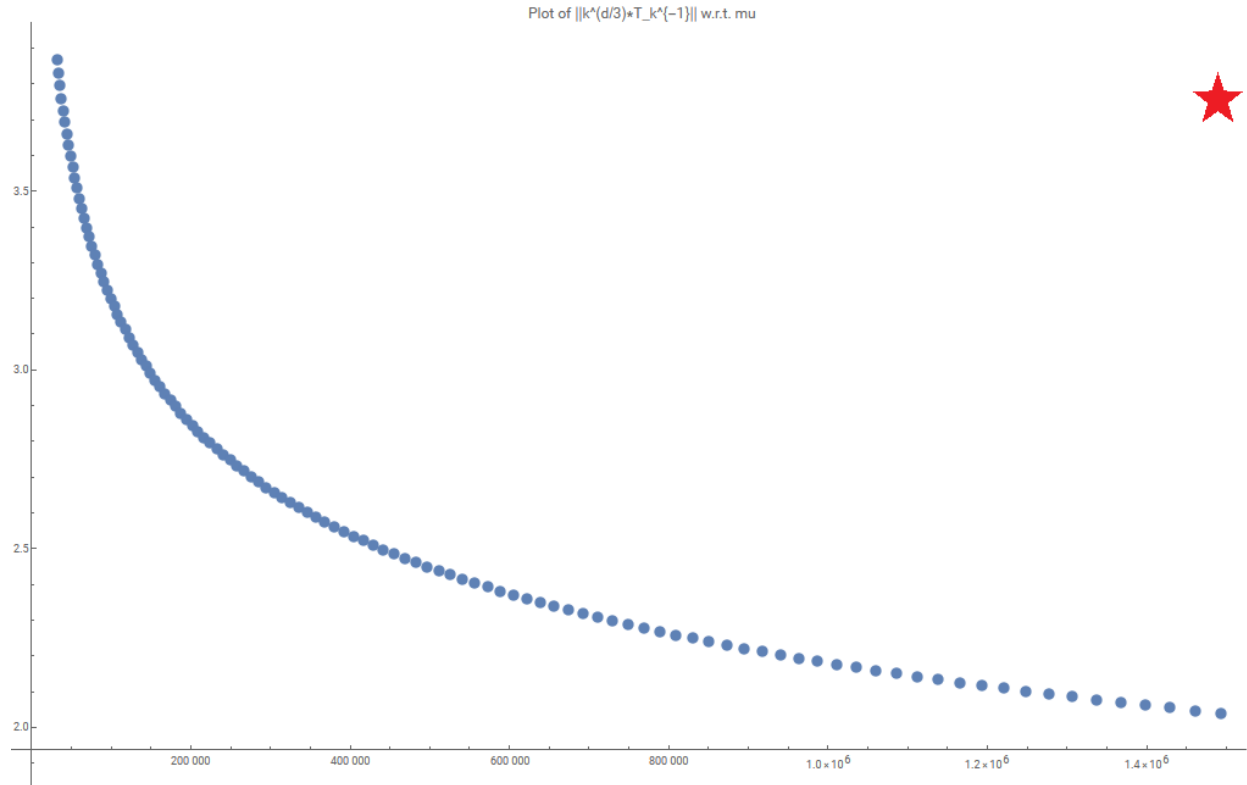


Figure 8: Plot presents upper bounds for $\|k^{d/3} \cdot T_k^{-1}\|_{B(\ell^1)}$ as a function of μ used in Theorem 3.17 for the case $\alpha \cdot h > \frac{1}{375}$, and $\mu \in [30000, 1.5 \cdot 10^6]$. The asymptotic bound for $\mu > \bar{\mu}$ in this case is equal to 3.74 – for comparison marked with the red star.